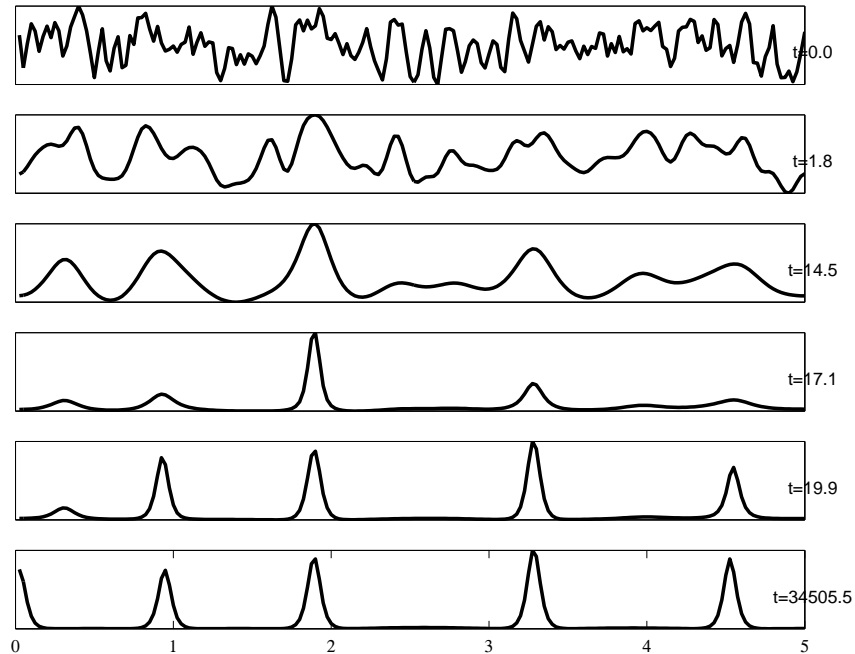


Localized structures, their stability and dynamics in PDEs

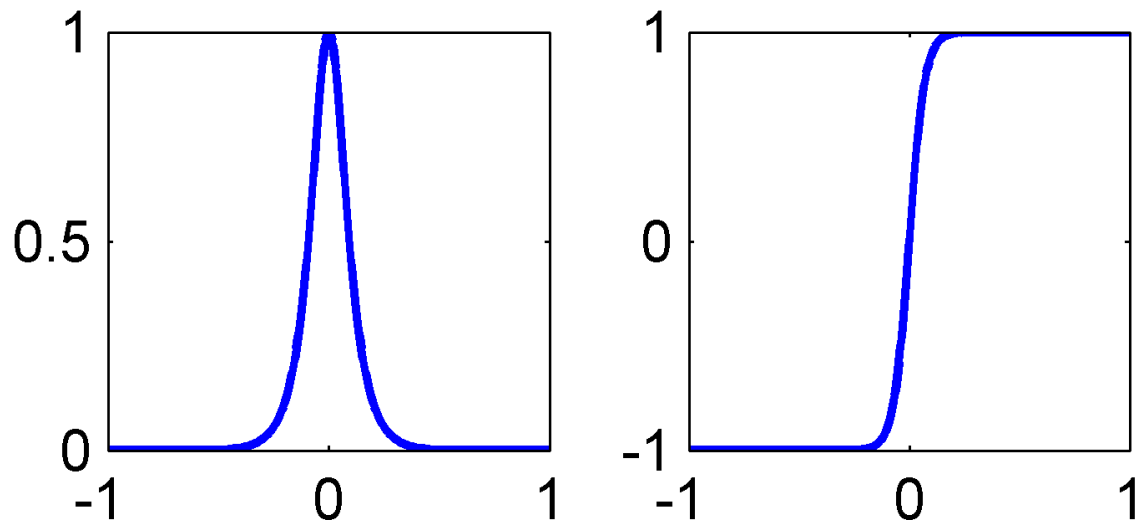


Theodore Kolokolnikov

Joint works with Michael Ward, Juncheng Wei, James Von Brecht, David Uminsky, Hui Sun, Andrea Bertozzi, Xiaofeng Ren, Mark Pavlovski, Rebecca McKay, David Iron, Thomas Erneux,

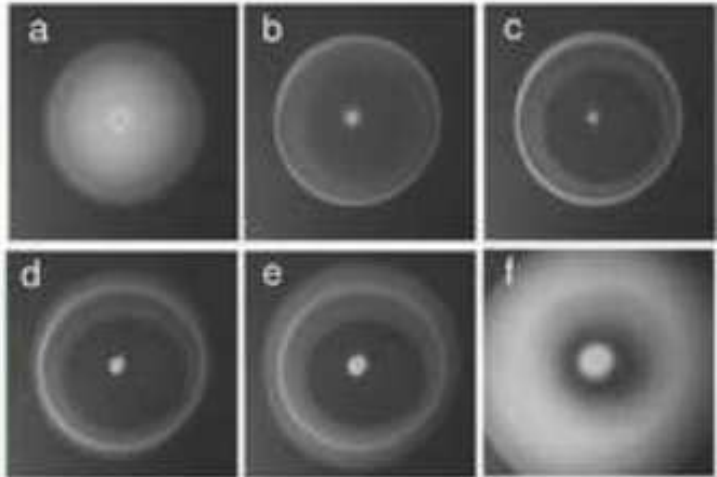
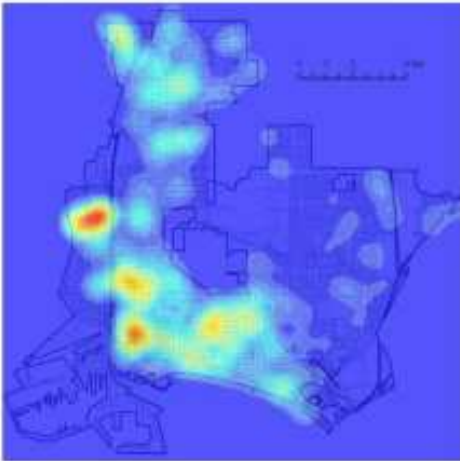
What are localized patterns?

- Regions of *sharp gradients* in the solution to PDEs
- Basic building block: either a spike or an interface



Examples from nature

seashells * fish * crime hotspots in LA * stressed bacterial colony

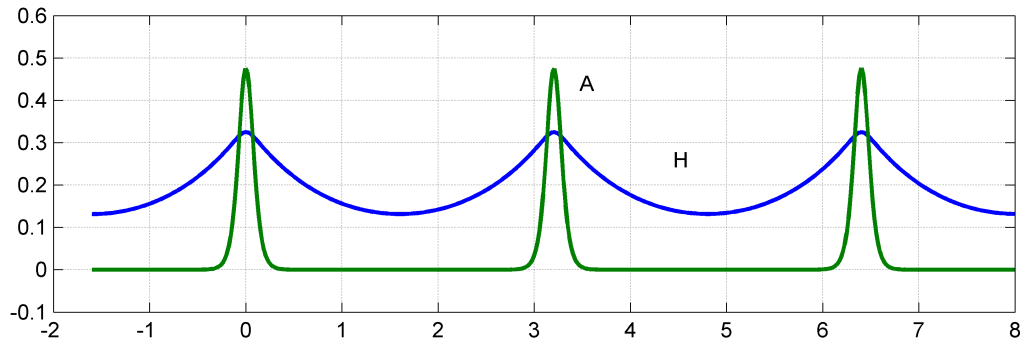


Classical Gierer-Meinhardt model

$$A_t = \varepsilon^2 \Delta A - A + \frac{A^2}{H}; \quad \tau H_t = D \Delta H - H + A^2$$

- Introduced in 1970's to model cell differentiation in hydra
- Mostly of mathematical interest: one of the simplest RD systems
- Has been intensively studied since 1990's [by mathematicians!]
- Key assumption: **separation of scales**

$$\varepsilon \ll 1 \text{ and } \varepsilon^2 \ll D.$$



- Roughly speaking, H is constant on the scale of A so the steady state looks "roughly" like $A(x) \sim Cw \left(\frac{x - x_0}{\varepsilon} \right)$ where

$$\Delta w - w + w^2 = 0.$$

- Questions: What about stability? What about location of the spike x_0 ?

“Classical” Results in 1D:

- Wei 97, 99, Iron+Wei+Ward 2000: Stability of K spikes in the GM model in one dimension
- Two types of possible instabilities: structural instabilities or translational instabilities
- Structural instabilities (large eigenvalues) lead to spike collapse in $O(1)$ time
- Translational instabilities can lead to “slow death”: spikes drift over large time scales
- **Main result 1:** There exists a sequence of thresholds D_K such that K spikes are stable iff $D < D_K$.
- **Main result 2:** Slow dynamics of K spikes is described by an ODE with $2K$ variables (spike heights and centers) subject to K algebraic constraints between these variables.

Large eigenvalues

- Careful derivation leads to a **nonlocal eigenvalue problem** (NLEP) of the form

$$\lambda\phi = \Delta\phi + (-1 + 2w)\phi - \chi w^2 \frac{\int w\phi}{\int w^2}; \quad \chi := \frac{4 \sinh^2\left(\frac{1}{\sqrt{D}}\right)}{2 \sinh^2\left(\frac{1}{\sqrt{D}}\right) + 1 - \cos[\pi(1 - 1/K)]}$$

- **Key theorem (Wei, 99):** $\text{Re}(\lambda) < 0$ iff $\chi < 1$
- **Corollary:** On a domain $[-1, 1]$, large eigenvalues are stable iff $D < D_{K,\text{large}}$ where

$$D_{K,\text{large}} = \frac{1}{\text{arcsinh}^2(\sin 2\pi/K)}$$

- When unstable, this can lead to **competition instability**.
- Movies: [stable](#); [unstable](#)

Small eigenvalues

- Causes a *very slow drift*
- Iron-Ward-Wei 2000: The slow dynamics of the system can be reduced to a coupled algebraic-differential system of ODEs
- Movie: [slow drift](#)

Two dimensions

- Structural stability is similar
- Dynamics [Ward et.al, 2000, K-Ward, 2004, K-Ward 2005]:

$$\frac{dx_0}{dt} \sim -\frac{4\pi\varepsilon^2}{\ln \varepsilon^{-1} + 2\pi R_0} \nabla R_0$$

where

$$R_0 = \lim_{x \rightarrow x_0} \left[G(x, x_0) + \frac{1}{2\pi} \ln(|x - x_0|) \right];$$

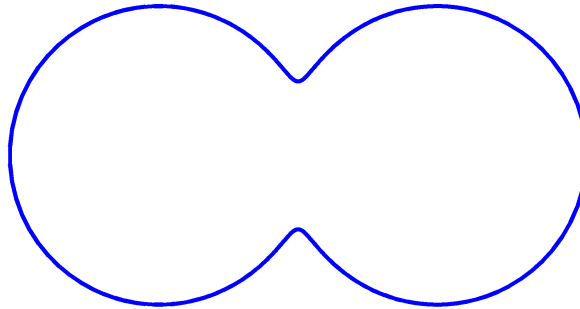
$$\nabla R_0 = \lim_{x \rightarrow x_0} \nabla_x \left[G(x, x_0) + \frac{1}{2\pi} \ln(|x - x_0|) \right];$$

$$\Delta G - \frac{1}{D}G = -\delta(x - x_0) \text{ on } \Omega; \quad \partial_n G = 0 \text{ on } \partial\Omega$$

- Equilibrium location x_0 satisfies $\nabla R_0 = 0$, occurs at the extremum of the regular part of the Neumann's Green's function

Dumbbell-shaped domain

- QUESTION: Suppose that a domain has a dumb-bell shape. Where will the spike drift??
- What are the possible equilibrium locations for a single spike?



Small D limit

- If D is very small, $R_0(x_0) \sim C(x_0) \exp\left(-\frac{1}{\sqrt{D}} |x_0 - x_m|\right)$ where x_m is the point on the boundary closest to x_0
- This means that R_0 is **minimized at the point furthest away from the boundary when $D \ll 1$**
 - In the limit $\varepsilon^2 \ll D \ll 1$, the spike drifts towards the point furthest away from the boundary.
 - For a dumbbell-shaped domain above, the three possible equilibria are at the "centers" of the dumbbells (stable) and at the center of the neck (unstable saddle point)
 - For multiple spikes, their locations solve "ball-packing problem".
- Movie: $D = 0.03, \varepsilon = 0.04$

Large D limit

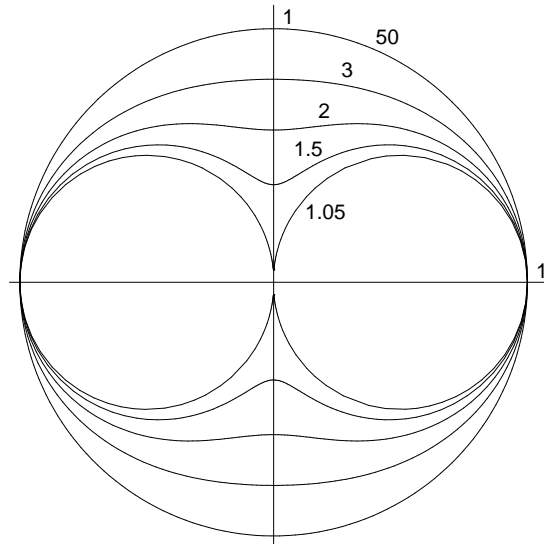
- We get the **modified Green's function**:

$$\Delta G_m - \frac{1}{|\Omega|} = -\delta(x - x_0) \text{ inside } \Omega, \quad \partial_n G = 0 \text{ on } \partial\Omega;$$

$$R_{m0} = \lim_{x \rightarrow x_0} \left[G_m(x, x_0) + \frac{1}{2\pi} \ln(|x - x_0|) \right].$$

- [K, Ward, 2003]: For a domain which is an analytic mapping of a unit disk, $\Omega = f(B)$, we derive an **exact formula** for ∇R_{m0} in terms of the residues of $f(z)$ outside the unit disk.

- Take $f(z) = \frac{(1 - a^2)z}{z^2 + a^2}$; $x_0 = f(z_0)$:



Then

$$\nabla R_{m0}(x_0) = \frac{\nabla s(z_0)}{f'(z_0)}$$

where

$$\nabla s(z_0) = \frac{1}{2\pi} \left(\begin{array}{l} \frac{z_0}{1-|z_0|^2} - \frac{(\bar{z}_0^2+3a^2)\bar{z}_0}{\bar{z}_0^4-a^4} + \frac{a^2\bar{z}_0}{\bar{z}_0^2a^2-1} + \frac{\bar{z}_0}{\bar{z}_0^2-a^2} \\ - \frac{(a^4-1)^2(|z_0|^2-1)(z_0+a^2\bar{z}_0)(\bar{z}_0^2+a^2)}{(a^4+1)(\bar{z}_0^2a^2-1)(z_0^2-a^2)(\bar{z}_0^2-a^2)^2} \end{array} \right)$$

- Corollary: for above Ω , ∇R_{m0} has a unique root at the origin!
 - In the limit $D \gg 1$, all spikes will drift towards the neck.
- Complex bifurcation diagram as D is increased.
- Movie: $\varepsilon = 0.05$, $D = 0.1$; $D = 1$.

”Huge” D

- In the limit $D \rightarrow \infty$, (Shadow limit), an interior spike is unstable and moves towards the boundary [Iron Ward 2000; Ni, Poláčik, Yanagida, 2001].
- For **exponentially large but finite** $D = O(\exp(-C/\varepsilon))$, boundary effects will compete with the Green’s function.
- [K, Ward, 2004]: Define

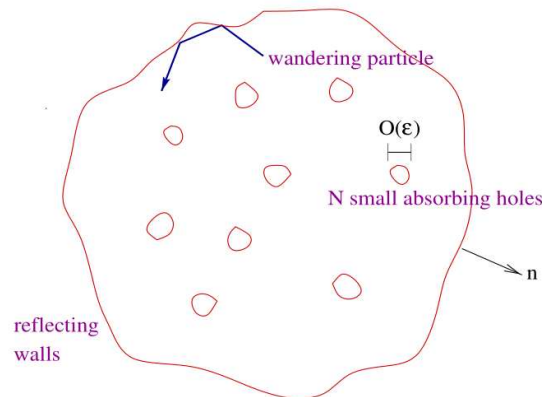
$$\sigma := \frac{\varepsilon}{2} \ln \left(\frac{C_0}{|\Omega|} D \varepsilon^{-1/2} \right); \quad C_0 \approx 334.80;$$

Then the spike will move towards the boundary whenever its distance from the closest point of the boundary is at most σ ; otherwise it will move away from the boundary.

- Movies: $\varepsilon = 0.05$, $D = 10$; $D = 100$

Related problem: Mean first passage time

- Question: Suppose you want to catch a fish in a lake covered by ice. Where do you drill a hole to maximize your chances?
- Related questions: cell signalling; oxygen transport in muscle tissues; cooling rods in a nuclear reactor...
- Consider N non-overlapping small "holes" each of small radius ε . A particle is performing a random walk inside the domain Ω . If it hits a hole, it gets destroyed; if it hits a boundary, it gets reflected. Question: what is the expected lifetime of the wandering particle? How do we place the holes to minimize this lifetime [i.e. catch the fish, cool the nuclear reactor...]?



- The expected lifetime is proportional to $1/\lambda$ where λ is the smallest eigenvalue of the problem:

$$\Delta u + \lambda u = 0 \text{ inside } \Omega \setminus \Omega_p; \quad u = 0 \text{ on } \partial\Omega_p; \quad \partial_n u = 0 \text{ on } \partial\Omega$$

where $\Omega_p = \bigcup_{i=1}^N \Omega_\varepsilon$.

- [K-Ward-Titcombe, 2005]: The smallest eigenvalue is given by

$$\lambda \sim \frac{2\pi N}{\ln \frac{1}{\varepsilon}} \left(1 - \frac{2\pi}{\ln \frac{1}{\varepsilon}} p(x_1, \dots, x_N) + O\left(\frac{1}{(\ln \frac{1}{\varepsilon})^2}\right) \right)$$

where

$$p(x_1, \dots, x_N) := \sum \sum G_{ij};$$

$$G_{ij} = \begin{cases} G_m(x_i, x_j) & \text{if } i \neq j \\ R_m(x_i, x_j) & \text{if } i = j \end{cases}$$

$$\Delta G_m(x, x') - \frac{1}{|\Omega|} = -\delta(x - x') \text{ inside } \Omega, \quad \partial_n G = 0 \text{ on } \partial\Omega;$$

$$R_m(x, x') = G_m(x, x') + \frac{1}{2\pi} \ln(|x - x'|).$$

- The optimum trap placement is at the minimum of $p(x_1, \dots, x_N)$
- **The answer is the same as for spike locations for GM model with $D \gg 1$!!**

Disk domain, N holes

We need to minimize

$$p(x_1 \dots x_N) = - \sum_{j \neq k} \ln |x_j - x_k| - \sum_{j,k} \ln |1 - x_j \bar{x}_k| + N \sum_j |x_j|^2$$

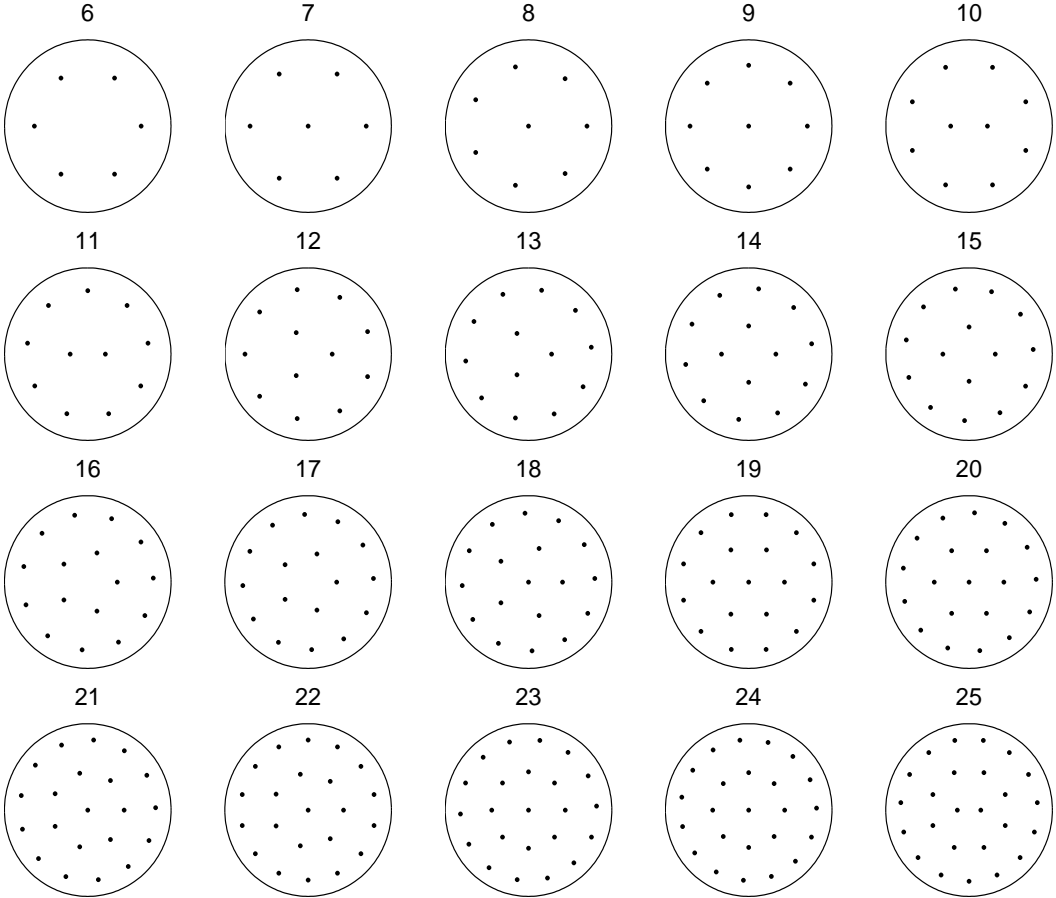
Particles on a ring: $x_k = r e^{ik2\pi/N}$. The min occurs when

$$\frac{r^{2N}}{1 - r^{2N}} = \frac{N - 1}{2N} - r^2$$

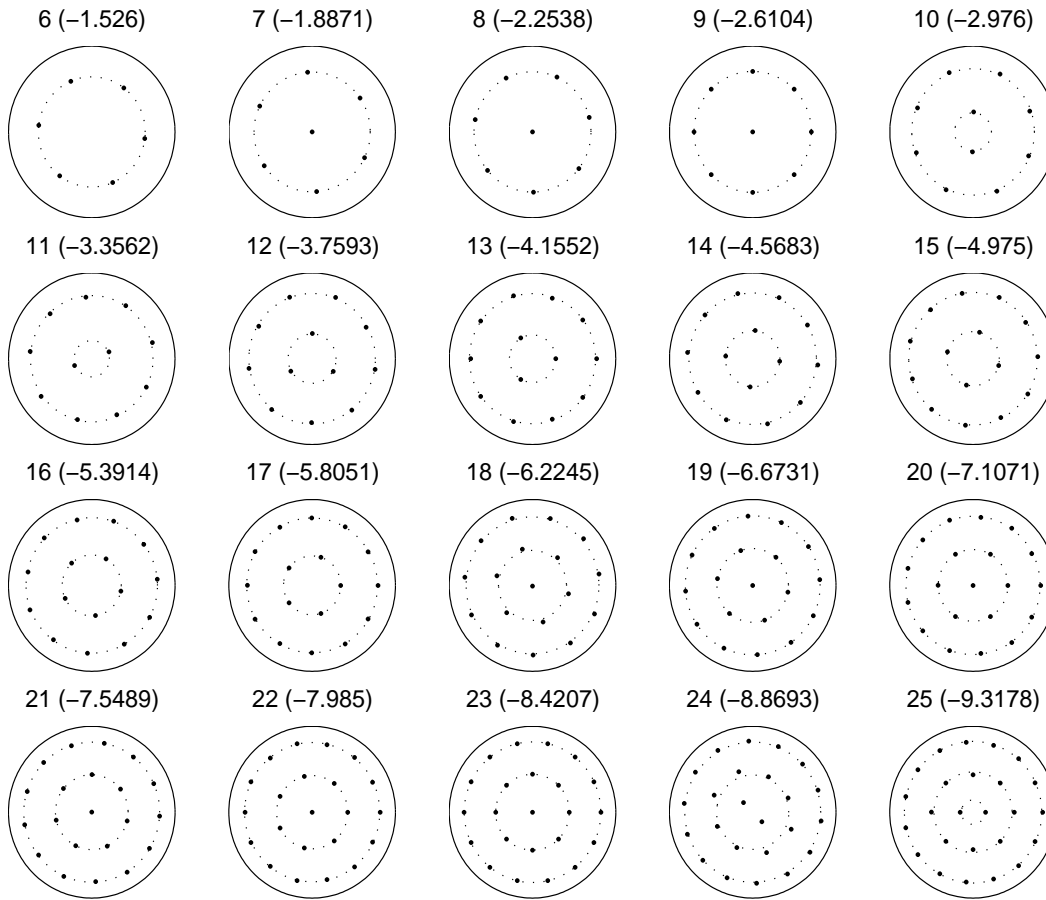
Note that $r \rightarrow 1/\sqrt{2}$ as $N \rightarrow \infty$; the optimal ring divides the unit disk into two equal areas.

Particles on 2,3,... m rings: Similar results are derived with complicated but numerically useful formulas.

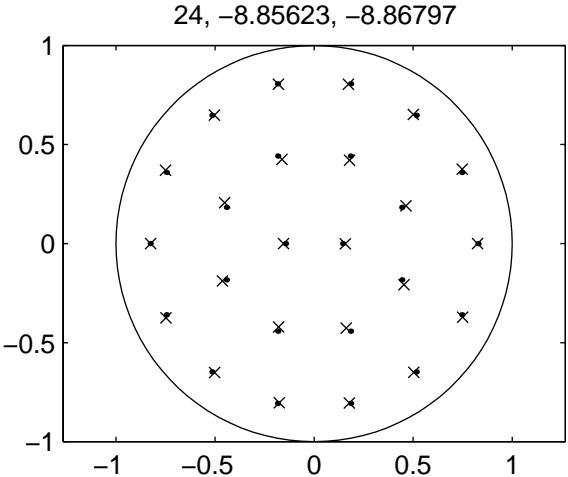
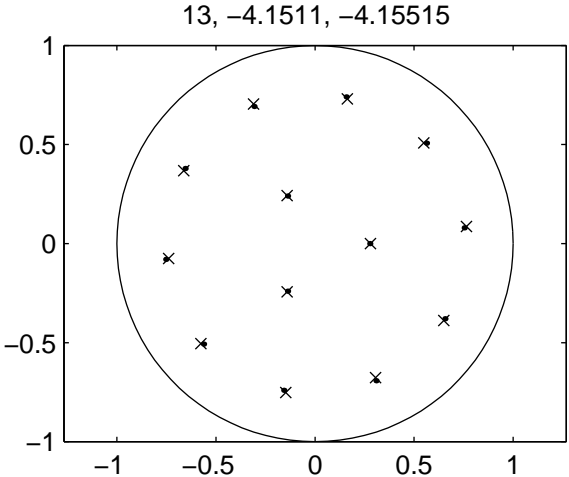
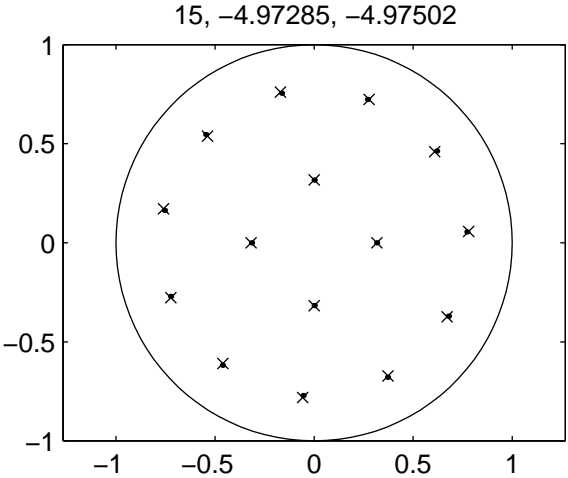
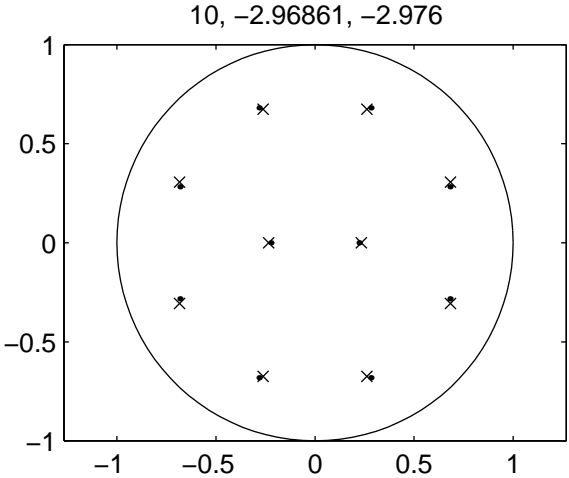
Constrained optimization on up to 3 rings



Full optimization of K traps

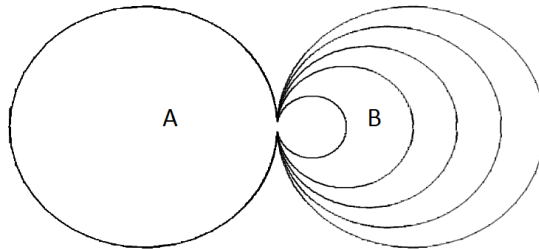


Comparison



Fishing on a dumbbell-shaped lake

- Question: can $R_m(x_0, x_0)$ have multiple minima?
 - Consider a domain consisting of two blobs of areas A, B connected at a single “bottleneck” point.



- When $A = B$, optimal place to catch fish is at the neck of the domain; only one minimum using complex variables method.
- If $\frac{1}{3} \leq \frac{A}{B} \leq 3$ then there is a minimum at the neck. If $A \gg B$ then the minimum is inside A . But when $\frac{A}{B}$ is just above 3, there is a complex bifurcation structure and multiple minima can exist!

Entire solutions to GM in higher dimensions

$$0 = \varepsilon^2 \Delta A - A + \frac{A^2}{H}; \quad 0 = \Delta H - H + A^2$$

- **Open question:** Does a spike solution exist in all of \mathbb{R}^3 ??
 - In 1D or 2D, there is separation of scales so YES. The inner problem is the ground state

$$\Delta w - w + w^2 = 0$$

- In 3D, the inner problem is **fully coupled**, the core problem becomes

$$0 = \Delta A - A + \frac{A^2}{H}; \quad 0 = \Delta H + A^2$$

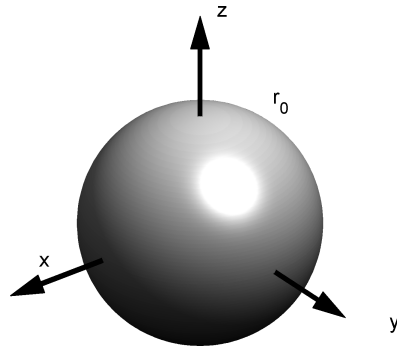
- No separation of scales in 3D. **Open question:** Does a spike in 3D exist???

Solutions concentrating on spheres in \mathbb{R}^3

- Consider a general GM model:

$$0 = \varepsilon^2 \Delta A - A + \frac{A^p}{H^q}; \quad 0 = \Delta H - H + \frac{A^m}{H^s}.$$

- [Ni-Wei 2006, K-Wei, 2006] Shell-solutions: Seek solutions where A concentrates on a surface of a sphere of radius r_0 .



$$A(x) \sim Cw \left(\frac{|x| - r_0}{\varepsilon} \right)$$

where w is the 1D ground state: $w_{yy} - w + w^2 = 0$; $w = \frac{3}{2} \operatorname{sech}^2(y/2)$.

- In 3D, the radius of the sphere satisfies

$$\frac{p-1}{q} \sim \frac{e^{2r_0} - 1 - r_0}{e^{2r_0} - 1} \quad \text{as } \varepsilon \rightarrow 0$$

- Note that $\frac{p-1}{q} \rightarrow 1$ as $r_0 \rightarrow \infty$.

- The "standard GM"

$$\varepsilon^2 \Delta A - A + A^2/H = 0 = \Delta H - H + A^2 \quad (1)$$

has $(p, q, m, s) = (2, 1, 2, 0)$ is a degenerate case ($p+1 = q, r_0 \rightarrow \infty$)

- [K-Wei, 2012] For (1) we have

$$\varepsilon \sim \exp(-2r_0) (1 + 2r_0) \frac{70}{103} \quad (2)$$

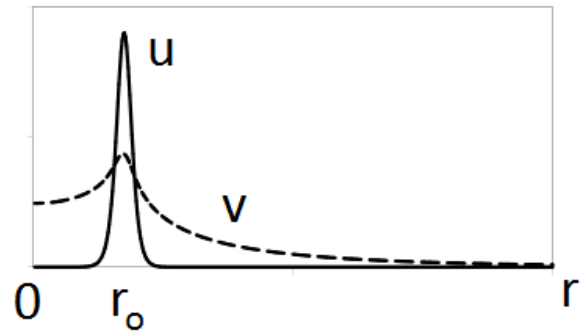
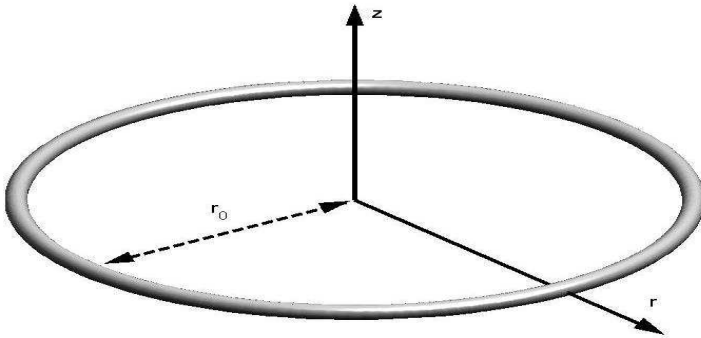
- The computation to get (2) is about 10 pages.

- Roughly, $r_0 \sim -\frac{1}{2} \ln \varepsilon \rightarrow \infty$ as $\varepsilon \rightarrow 0$.

Smoke-ring solutions

Axi-symmetric ansatz:

$$A(x, y, z) = u(r, z), \quad H(x, y, z) = v(r, z) \quad \text{where } r = \sqrt{x^2 + y^2}$$



The GM model becomes:

$$0 = \varepsilon^2 \left(\Delta_{(r,z)} u + \frac{1}{r} u_r \right) - u + \frac{u^p}{v^q}; \quad 0 = \left(\Delta_{(r,z)} v + \frac{1}{r} v_r \right) - v + \frac{u^m}{v^s} \quad (3)$$

Theorem Suppose that $q = p - 1$. Then the (3) admits a solution of the form

$$u \sim Cw(R); \quad R = \frac{\sqrt{(r - r_0)^2 + z^2}}{\varepsilon}$$

where w is a 2D ground state:

$$w_{RR} + \frac{1}{R}w_R - w + w^p = 0; \quad w'(0) = 0; \quad w > 0$$

and the radius r_0 given implicitly by

$$1 - 2r_0 \int_0^1 \frac{e^{-2r_0 t}}{\sqrt{1-t^2}} dt = \frac{1}{2}(m - s - 1) \frac{\int_0^\infty w^m \left(\int_0^R w^{p+1} t dt \right) R dR}{\left(\int_0^\infty w^m R dR \right) \left(\int_0^\infty w^{p+1} R dR \right)}. \quad (4)$$

The solution to (4) is always unique It exists if $m - s - 1 \leq 2$.

Some key steps in derivation

- Need to compute the axi-symmetric Green's function:

$$\Delta G + \frac{1}{r}G_r - G = -\delta(x, x_0).$$

- **Descent from 3D:** G is a convolution of the 3D Green's function $\Gamma(x, x') = \frac{e^{-|x-x'|}}{4\pi|x-x'|}$ along a ring of radius r_0 :

$$G(r, z, r_0, z_0) = \frac{r_0}{4\pi} \int_0^{2\pi} \frac{\exp[-(r^2 + r_0^2 - 2rr_0 \cos \omega + (z - z_0)^2)^{1/2}]}{4\pi(r^2 + r_0^2 - 2rr_0 \cos \omega + (z - z_0)^2)^{1/2}} d\omega$$

- Asymptotically **expand the singular integral** as $r \rightarrow r_0$
- Expand the steady state in **two scales:** ε and $\ln \varepsilon$.
- Higher-order solvability condition at $O(\varepsilon \ln \varepsilon)$.

Perturbed Allen-Cahn model

$$u_t = \varepsilon^2 \Delta u - 2(u - \varepsilon a)(u - 1)(u + 1), \quad x \in \Omega \subset \mathbb{R}^2; \quad \partial_n u = 0 \text{ on } \partial\Omega$$

- When $a = 0$, solution consists of an **interface** whose evolution tries to minimize its diameter. Equilibrium solution has zero curvature.
- When $a \neq 0$, the evolution of the equilibrium solution has a curvature \hat{R}^{-1} where $\hat{R} = \frac{1}{2a}$.
 - Sometimes the interface gets stuck in a narrow channel, other times it passes through.
 - In [K-iron-Rumsey-Wei, 2008] we classify the stability of such an interface.
 - [Movie: stuck](#) [Movie: unstuck](#)
 - Main result: Eigenvalues satisfy the **geometric eigenvalue problem**,

$$\begin{cases} w_{zz} - \hat{R}^{-2}w = -\lambda_0 w; \\ w'(-l/2) + \kappa_- w(-l/2) = 0; \\ w'(l/2) + \kappa_+ w(l/2) = 0; \end{cases}$$

where l is the interface length; κ_- , κ_+ are the two curvatures of the boundary at the points where the interface intersects it.

Layer oscillations

- FitzHuhg-Nagumo type model:

$$u_t = \varepsilon^2 u_{xx} + 2(u - u^3) + w, \quad \tau w_t = Dw_{xx} - u + \beta$$

Neumann BC on $[0, 1]$

$$\varepsilon \ll 1, \quad D \gg 1$$

- Stationary steady state is an interface computed from the shadow limit $D \rightarrow \infty$

$$w \sim 0; \quad u \sim \tanh\left(\frac{l_0 - x}{\varepsilon}\right); \quad l_0 := (1 + \beta)/2$$

- [McKay-K]: As τ is increased, the interface is destabilized via a Hopf Bifurcation ([movie1](#), [movie2](#)). The critical scaling is:

$$\tau = \frac{D}{\varepsilon} \tau_0, \quad \text{where } \tau_0 = O(1).$$

- The interface position is given by

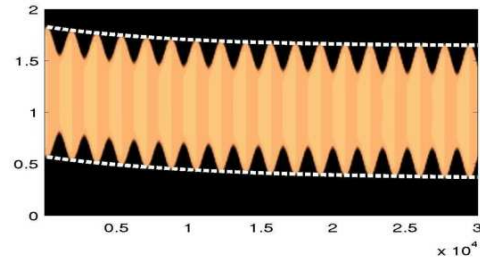
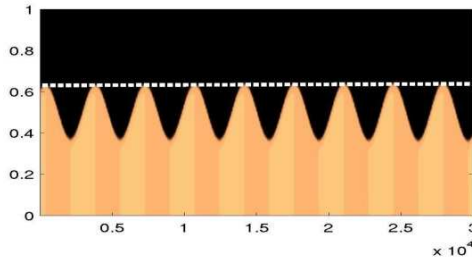
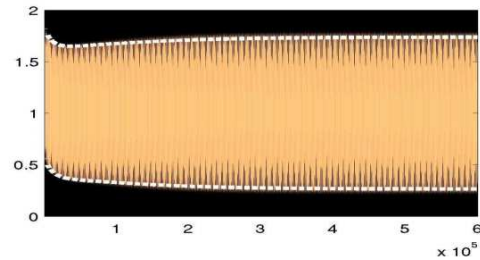
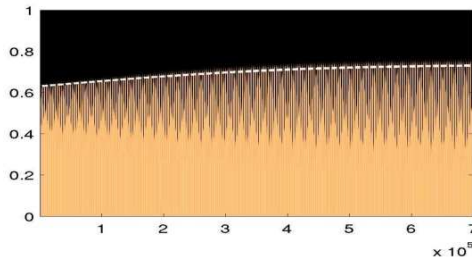
$$l(t) \sim l_0 + A(t) \cos(\sqrt{3/\tau_0 \varepsilon} D^{-1/2} t + \phi_0)$$

where A is the oscillation envelope that satisfies

$$\frac{D dA}{\varepsilon dt} = \left(\frac{1}{4}(1 - 3\beta^2) - \frac{1}{8\tau_0} \right) A - \frac{3}{4} A^3.$$

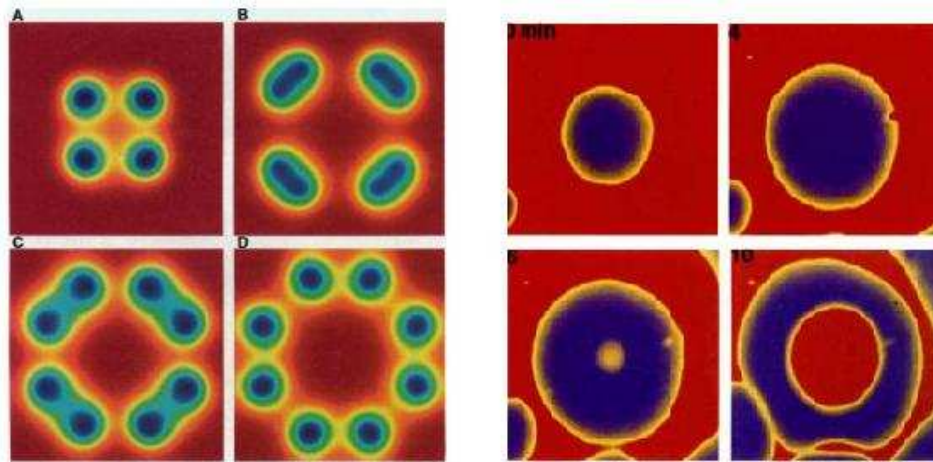
- Hopf bifurcation occurs when

$$\tau_{0h} = \begin{cases} \frac{1}{2(1-3\beta^2)} & \text{if } |\beta| < 3^{-1/2}; \\ \infty & \text{otherwise} \end{cases}.$$



Self-replication

- In 1993, Pearson reported self-replicating spots in the Gray-Scott model [J.E. Pearson, Science, 261, 189 (1993)].
- Experiments using Ferrocyanide-iodate-sulphite reaction (which GS models) confirmed numerical observation [Lee et.al, Nature, 1994].



Pearson (1993, numerics)

Lee et.al. (1994, lab)

- Self-replication was found in many other models, including chemical reactions, material science and nonlinear optics.

Gray-scott model

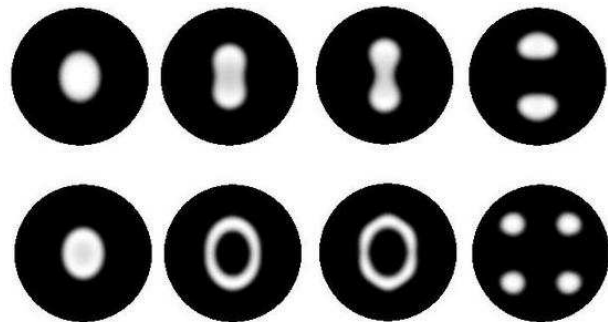
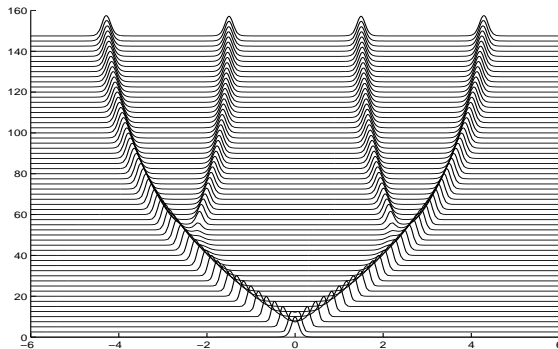
- Models a chemical reaction
- Large literature starting from 1990's: Doelman, Kaper, Muratov, Nishiura....

$$\begin{cases} u_t = D_v \Delta u - (F + k)u + vu^2 \\ v_t = D_u \Delta v + F(1 - v) + vu^2 \end{cases}$$

- Self-replication reduces to study a **fully-coupled 4-th order ODE:**

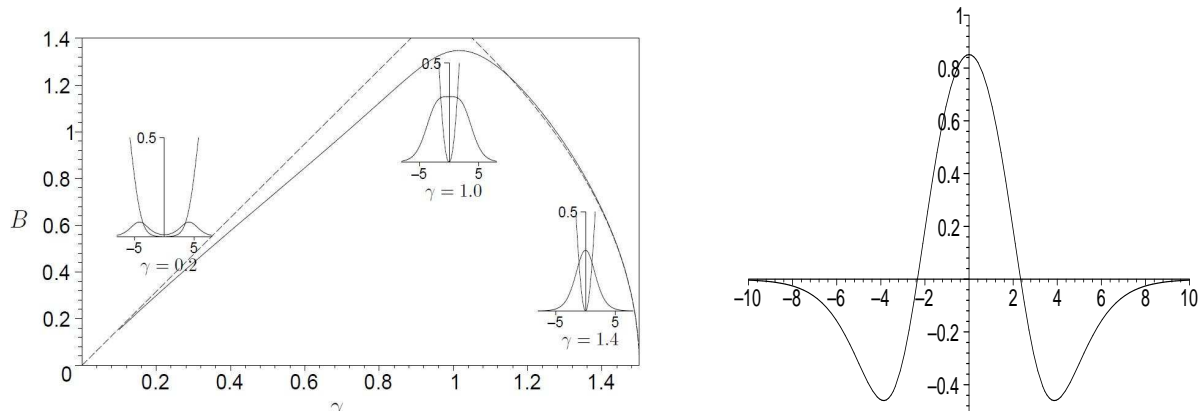
$$\begin{cases} \Delta U - U + U^2 V = 0 \\ \Delta V - U^2 V = 0 \\ V'(0) = 0 = U'(0), \quad V'(\infty) = B \end{cases}$$

- Replication has been observed in 1D and 2D (two different types):



Criteria for self-replication

- Four criteria, proposed by Nishiura and Ueyema (1999):
 1. The disappearance of the ground-state solution due to a fold point.
 2. The existence of a **dimple eigenfunction** at the fold point, responsible for the initiation of the self-replication process.
 3. Stability of the steady-state solution on one side of the fold point.
 4. The alignment (or cascade) of the fold points for K spots.
- Verification of these conditions is usually done numerically
- Analytic verification is an open problem for the GS model; order too high.



Simpler self-replication model in \mathbb{R}^N

$$u_t = \Delta u - u + \frac{(1 + a|x|^q) u^p}{\int_{\mathbb{R}^N} (1 + a|x|^q) u^{p+1}}; \quad \nabla u(0, t) = 0 \quad (5)$$

- Steady state satisfies (after rescaling):

$$0 = u_{rr} + \frac{N-1}{r} u_r - u + (1 + ar^q) u^p; \quad u'(0) = 0, \quad u > 0 \quad (\text{ss})$$

- Existence of ground state depends on a, q, p
- **Main result:** Self-replication occurs if a is gradually increased from 0, provided that

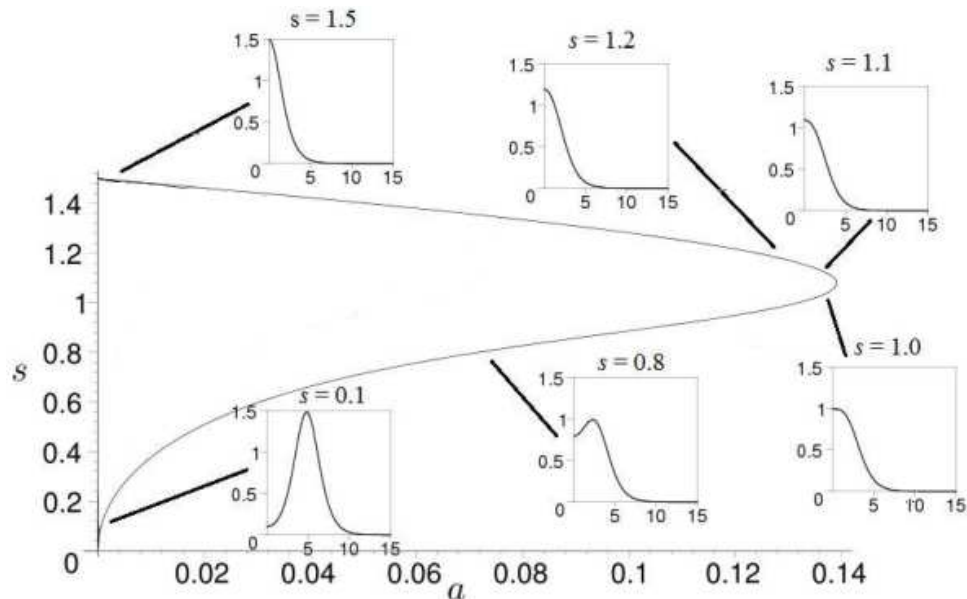
$$p > 1 \text{ and } q > \frac{(p-1)N}{2} \text{ if } N = 1 \text{ or } 2$$
$$1 < p < \frac{N+2}{N-2} \text{ and } q > \frac{(p-1)(N-1)}{2} \text{ if } N \geq 3.$$

Example: Bifurcation structure in 1-D

$$0 = u_{rr} - u + (1 + ar^2) u^2; \quad u'(0) = 0, \quad u > 0$$

- Two-bump solution connects to one-bump solution in a fold-point bifurcation. This is the **first condition for self replication**.

$$s := u(0; a)$$



Bifurcation structure in 3D

$$0 = u_{rrr} + \frac{2}{r}u_r - u + (1 + ar^q)u^2; \quad u'(0) = 0, \quad u > 0$$

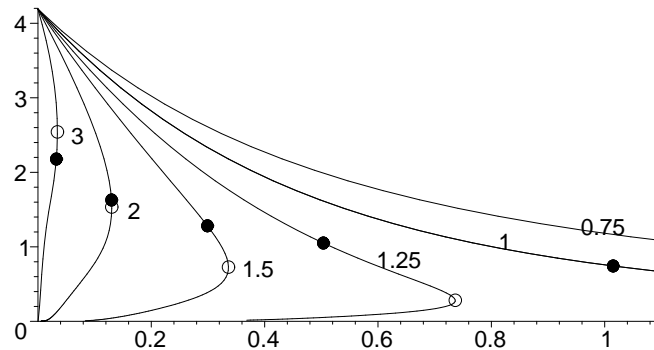
- If $q > 1$, there is a solution with $a \ll 1$, $u(0) \ll 1$ given by

$$u(r) \sim Cw(r - r_0) \quad \text{where} \quad r_0 = \left(\frac{1}{a}\right)^{1/q} \left(\frac{1}{q-1}\right)^{1/q}$$

where $w'' - w + w^p = 0$ is a 1-D ground state, C some constant.

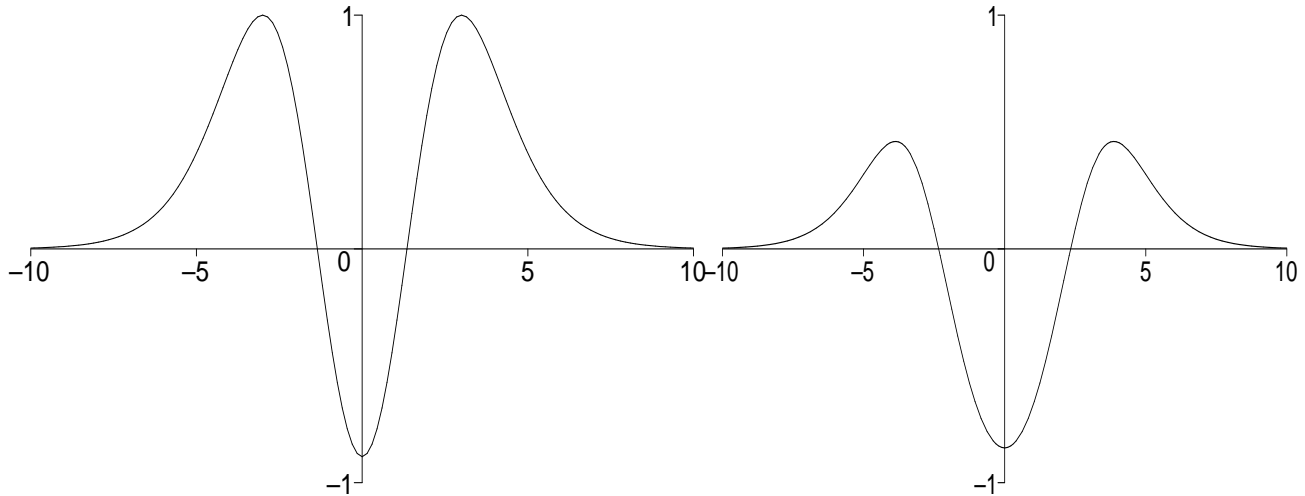
- If $q < 1$, there is a solution for $a \gg 1$ (no fold point)
- If $q = 1$, there is a solution with $a \gg 1$, $u(0) \ll 1$ given by

$$u(r) \sim Cw(r - r_0) \quad \text{where} \quad r_0 = O(\ln a)$$



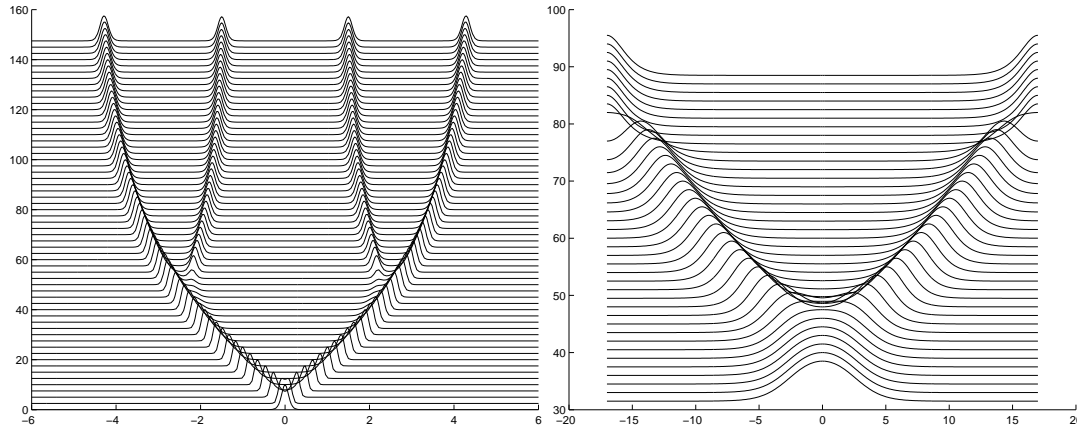
$p = 2$, q as indicated

- **Theorem:** There is a fold point when $q > 1$; no fold point if $q = 1$.
- **Theorem:** *The eigenfunction at the fold point has a dimple shape.* This verifies Nishiura-Ueyema condition 2



Dimple eigenvalue for simplified model (left) and for GS model (right)

Comparison with GS model



Left: GS model ([movie](#)). Right: Simplified model ([movie](#)).

- GS model: a cascade of self-replication events, resulting in multiple interior spikes.
- Simplified model: only one self-replication event; the spike moves to and merges with the boundary.
- Initial stages of self-replication mechanism are similar for the two models.

Nonradial stability ($N = 3$)

- Using spherical coordinates we decompose

$$Z(x, y, z) = \Phi(r)Y_l^m(\theta, \phi); \quad l = 0, 1, \dots; \quad m = 0, \pm 1 \dots \pm l$$

where Y_l^m are the spherical harmonics.

- For $l \geq 2$, The nonlocal term in (NLEP) disappears since $\int hZu^{p-1} = 0$, $l \geq 2$ and we get

$$\lambda_l \Phi = \Phi_{rr} + \frac{2}{r}\Phi_r - \frac{\gamma}{r^2}\Phi - \Phi + phu^{p-1}\Phi; \quad \gamma = l(l+1), \quad l \geq 2. \quad (\text{NREP})$$

- In the threshold case $q = p - 1$ and $a \gg 1$,

$$u(r) \sim Cw(r - r_0) \quad \text{where } r_0 = O(\ln a)$$

so that (NREP) becomes (LEP):

$$\lambda_l \Phi \sim \Phi_{rr} - \Phi + phu^{p-1}\Phi$$

which is **unstable!**

- Non-radial instability leads to **peanut-splitting**. [Click for movie](#)

UCLA Model of hot-spots in crime

- Recently proposed by Short Brantingham, Bertozzi et.al [2008].
- Very "sexy" math: e.g. *The New York Times*, Dec 2010, *Times top 50 ideas*, 2011
- Crime is ubiquitous but not uniformly distributed
 - some neighbourhoods are worse than others, leading to crime "hot spots"
 - Crime hotspots can persist for long time.



Fig. 1. Dynamic changes in residential burglary hotspots for two consecutive three-month periods beginning June 2001 in Long Beach, CA. These density maps were created using ArcGIS.

Figure taken from Short et.al., *A statistical model of criminal behaviour*, 2008.

- Crime is temporally correlated:
 - Criminals often return to the spot of previous crime
 - If a home was broken into in the past, the likelihood of subsequent breakin increases
 - Example: graffitti "tagging"

- Two-component model

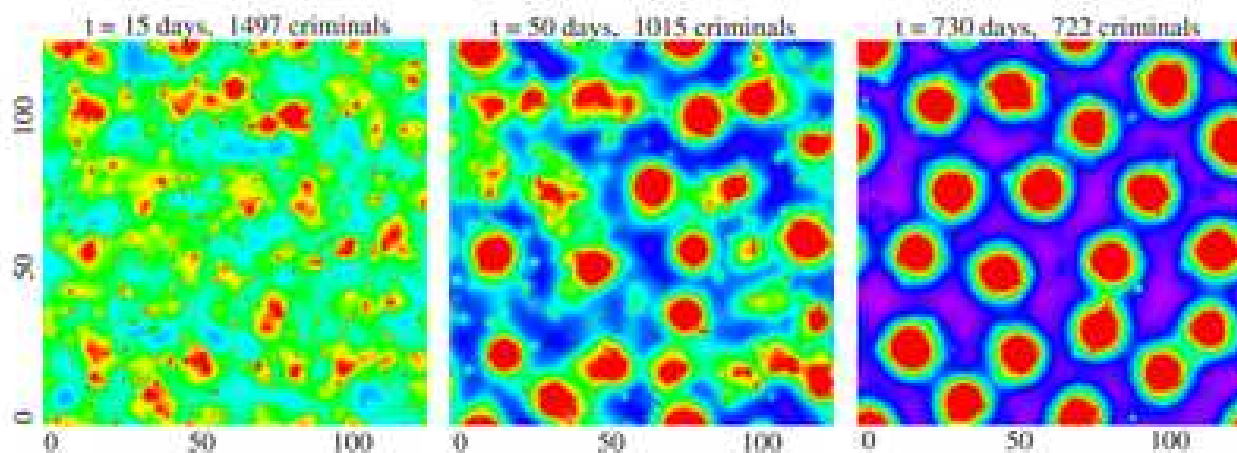
$$A_t = \varepsilon^2 A_{xx} - A + \rho A + \alpha$$

$$\tau \rho_t = D \left(\rho_x - 2 \frac{\rho}{A} A_x \right)_x - \rho A + \gamma - \alpha.$$

- $\rho(x, t) \equiv$ density of criminals;
- $A(x, t) \equiv$ "attractiveness" of area to crime
- $\alpha = O(1) \equiv$ "baseline attractiveness"
- $D(-2\frac{\rho}{A}A_x)_x$ models the motion of criminals towards higher attractiveness areas
- $\gamma - \alpha > 0$ is the baseline criminal "feed rate"
- We assume here:

$$\varepsilon^2 \ll 1$$

Numerical results: hot-spots forming



Taken from paper by Short, D'Orsogna, Pasour, Tita, Brantingham, Bertozzi and Chayes, M3AS 2008

Hot-spot steady state

$$0 = \varepsilon^2 A_{xx} - A + \rho A + \alpha; \quad 0 = D \left(\rho_x - 2 \frac{\rho}{A} A_x \right)_x - \rho A + \gamma - \alpha$$

- Key trick: $\rho_x - 2 \frac{\rho}{A} A_x = A^2 (\rho A^{-2})_x$.
- This suggests the change of variables:

$$v = \frac{\rho}{A^2};$$

so that

$$0 = \varepsilon^2 A_{xx} - A + v A^3 + \alpha; \quad 0 = D (A^2 v_x)_x - v A^3 + \gamma - \alpha. \quad (6)$$

- “Shadow limit” Large D : $v(x) \sim v_0$;

$$\varepsilon^2 A_{xx} - A + vA^3 + \alpha = 0; \quad v_0 \int_0^l A^3 dx = (\gamma - \alpha) l.$$

- $A \sim v_0^{-1/2} w(y)$, $y = x/\varepsilon$ where w is the ground state,

$$w_{yy} - w + w^3 = 0, \quad w'(0) = 0, \quad w \rightarrow 0 \text{ as } |y| \rightarrow \infty;$$

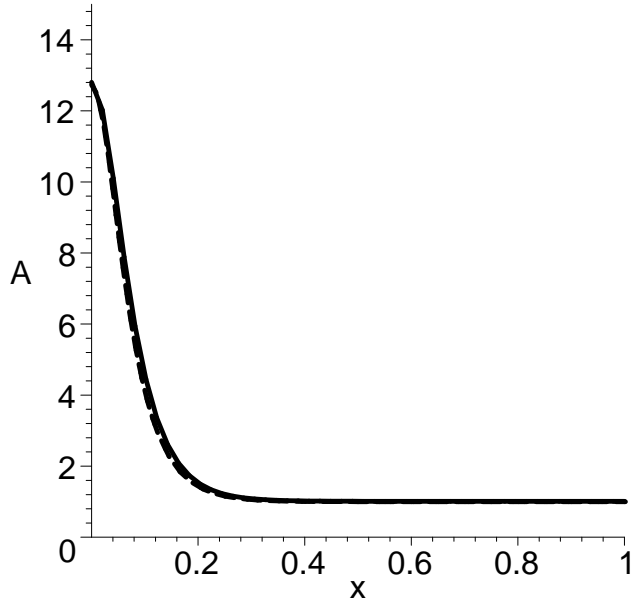
i.e.

$$w(y) = \sqrt{2} \operatorname{sech}(y)$$

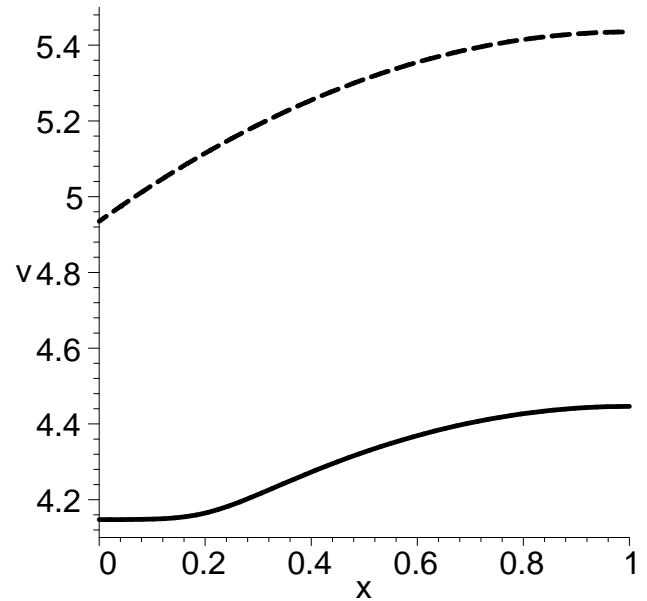
then

$$v_0 \sim \frac{\left(\int_{-\infty}^{\infty} w^3 dy\right)^2}{4l^2 (\gamma - \alpha)^2} \varepsilon^2;$$

$$A(x) \sim \begin{cases} \frac{2l(\gamma - \alpha)}{\varepsilon \int w^3} w(x/\varepsilon), & x = O(\varepsilon) \\ \alpha, & x \gg O(\varepsilon). \end{cases}$$



(a)



(b)

Figure 1: Steady state in one dimension. Parameter values are $D_0 = 1, \varepsilon = 0.05, \alpha = 1, \gamma = 2, x \in [0, 1]$. (a) The solid line is the steady state solution $A(x)$ of (6) computed by solving the associated boundary value problem numerically. The dashed line corresponds to the first-order composite approximation. (b) The solid line is the steady state solution for $v(x)$. Note the “flat knee” region within the spot center. The dashed line is the asymptotics result.

Stability of hot-spots (1D)

- **Localized states [preprint]:** Consider a periodic pattern consisting of *localized* hotspots of radius l . It is stable iff $l > l_c$ where

$$l_c := \frac{\varepsilon^{1/2} D^{1/4} \pi^{1/2} \alpha^{1/2}}{(\gamma - \alpha)^{3/4}}.$$

- **Turing instability in the limit $\varepsilon \rightarrow 0$:**

- Equilibrium steady state $A = \gamma$, $\rho = (\gamma - \alpha)/\gamma$ is Turing-unstable provided that

$$\gamma > \frac{3}{2}\alpha, \quad \varepsilon \rightarrow 0$$

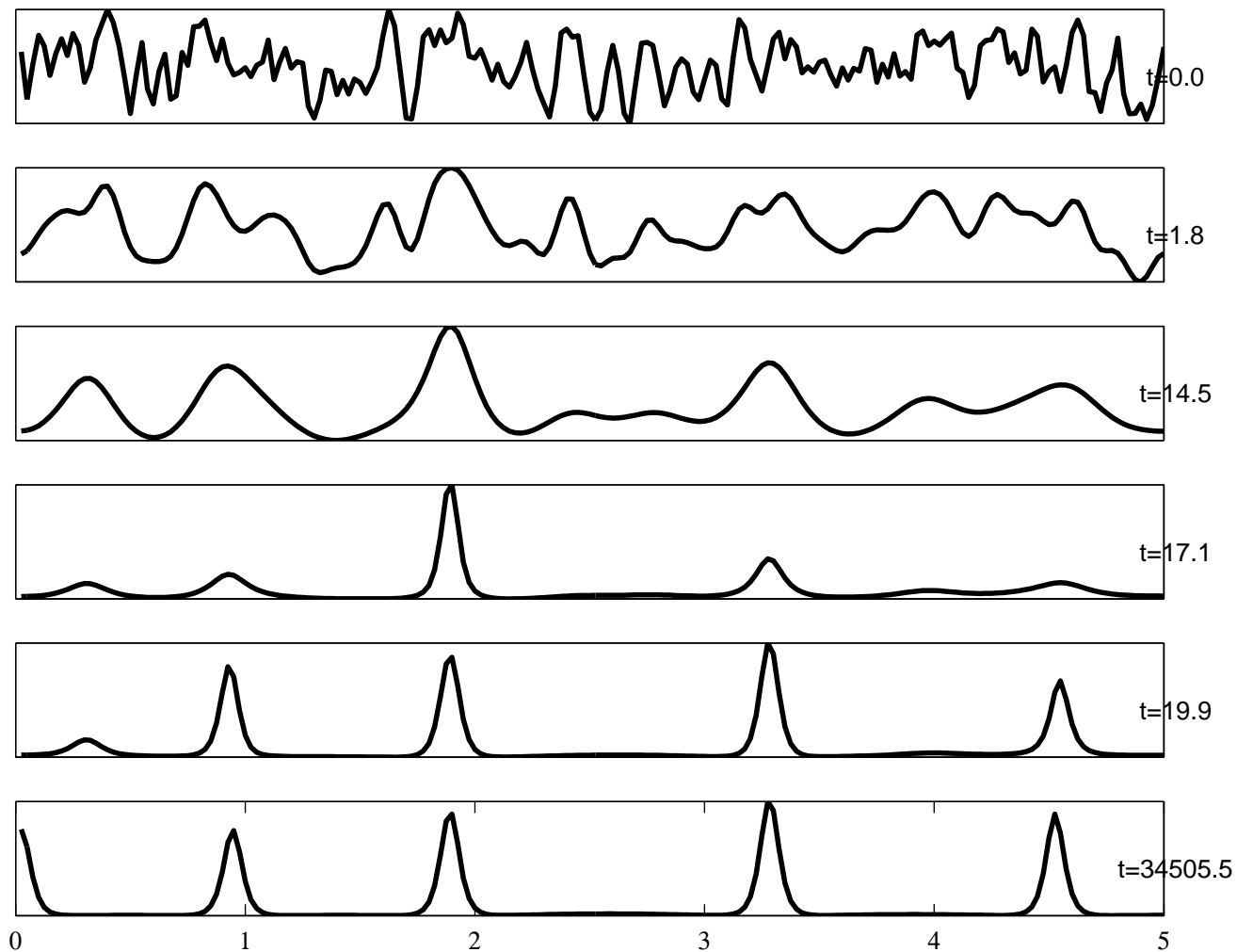
- **Preferred Turing characteristic length:**

$$l_{\text{turing}} \sim \varepsilon^{1/2} \frac{D^{1/4} 2\pi \sqrt{\gamma}}{(\gamma - A^0)^{1/4} (3\gamma^2 + 4\gamma - 6\alpha)^{1/4}}$$

- Note that both $O(l_c) = O(l_{\text{turing}}) = O(\varepsilon^{1/2})!$

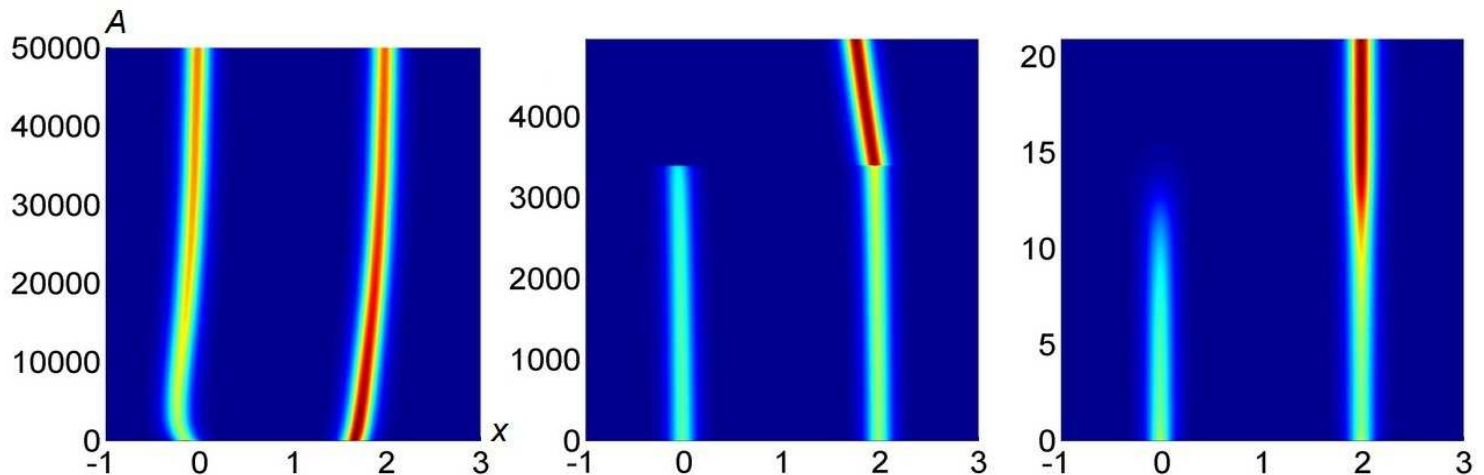
Example: $\alpha = 1$, $\gamma = 2$, $D = 1$, $\varepsilon = 0.03$.

Then $l_{turing} = 0.60$; $l_c = 0.13 < l_{turing}$



Small and large eigenvalues

- Near-translational invariance leads to “small eigenvalues (perturbation from zero)” corresponding eigenfunction is $\phi \sim w'$.
- Large eigenvalues are responsible for “competition instability”.
- Small eigenvalues become unstable before the large eigenvalues.
- Example: Take $l = 1, \gamma = 2, \alpha = 1, K = 2, \varepsilon = 0.07$. Then $D_{c,\text{small}} = 20.67, D_{c,\text{large}} = 41.33$.
 - if $D = 15 \implies$ two spikes are stable
 - if $D = 30 \implies$ two spikes have very slow developing instability
 - if $D = 50 \implies$ two spikes have very fast developing instability



Stability: large eigenvalues

- **Step 1:** Reduces to the nonlocal eigenvalue problem (NLEP):

$$\lambda\phi = \phi'' - \phi + 3w^2\phi - \chi \left(\int w^2\phi \right) w^3 \quad \text{where } w'' - w + w^3 = 0. \quad (7)$$

with

$$\chi \sim \frac{3}{\int_{-\infty}^{\infty} w^3 dy} \left(1 + \varepsilon^2 D \left(1 - \cos \frac{\pi k}{K} \right) \frac{\alpha^2 \pi^2}{4l^4 (\gamma - \alpha)^3} \right)^{-1}$$

- **Step 2: *Key identity*:** $L_0 w^2 = 3w^2$, where $L_0 \phi := \phi'' - \phi + 3w^2 \phi$. Multiply (7) by w^2 and integrate to get

$$\lambda = 3 - \chi \int w^5 = 3 - \chi \frac{3}{2} \int w^3$$

Conclusion: (7) is stable iff $\chi > \frac{2}{\int w^3} \iff D > D_{c,\text{large}}$.

- This NLEP in 1D can be fully solved!!

Stability: small eigenvalues

- Compute asymmetric spikes
- They bifurcate from symmetric branch
- The bifurcation point is precisely when $D = D_{c,\text{small}}$.
- This is “cheating”... but it gets the correct threshold!!

Stability of K spikes

- Possible boundary conditions:

Config type	Boundary conditions for ϕ
Single interior spike on $[-l, l]$ even eigenvalue	$\phi'(0) = 0 = \phi'(l)$
Single interior spike on $[-l, l]$ odd eigenvalue	$\phi(0) = 0 = \phi(l)$
Two half-spikes at $[0, l]$	$\phi'(0) = 0 = \phi(l)$
K spikes on $[-l, (2K - 1)l]$, Periodic BC	$\phi(l) = z\phi(-l), \quad \phi'(l) = z\phi'(-l),$ $z = \exp(2\pi ik/K), \quad k = 0 \dots K - 1$
K spikes on $[-l, (2K - 1)l]$, Neumann BC	$\phi(l) = z\phi(-l), \quad \phi'(l) = z\phi'(-l),$ $z = \exp(\pi ik/K), \quad k = 0 \dots K - 1$

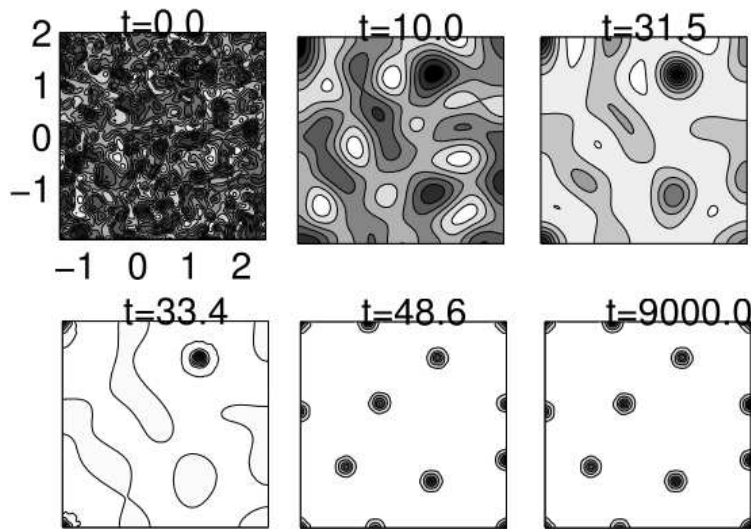
(same BC for ψ)

Two dimensions

Given domain of size S , let

$$K_c := 0.07037 \varepsilon^{-3/4} D^{-1/3} \left(\ln \frac{1}{\varepsilon} \right)^{1/3} (\gamma - \alpha) \alpha^{-2/3} S. \quad (8)$$

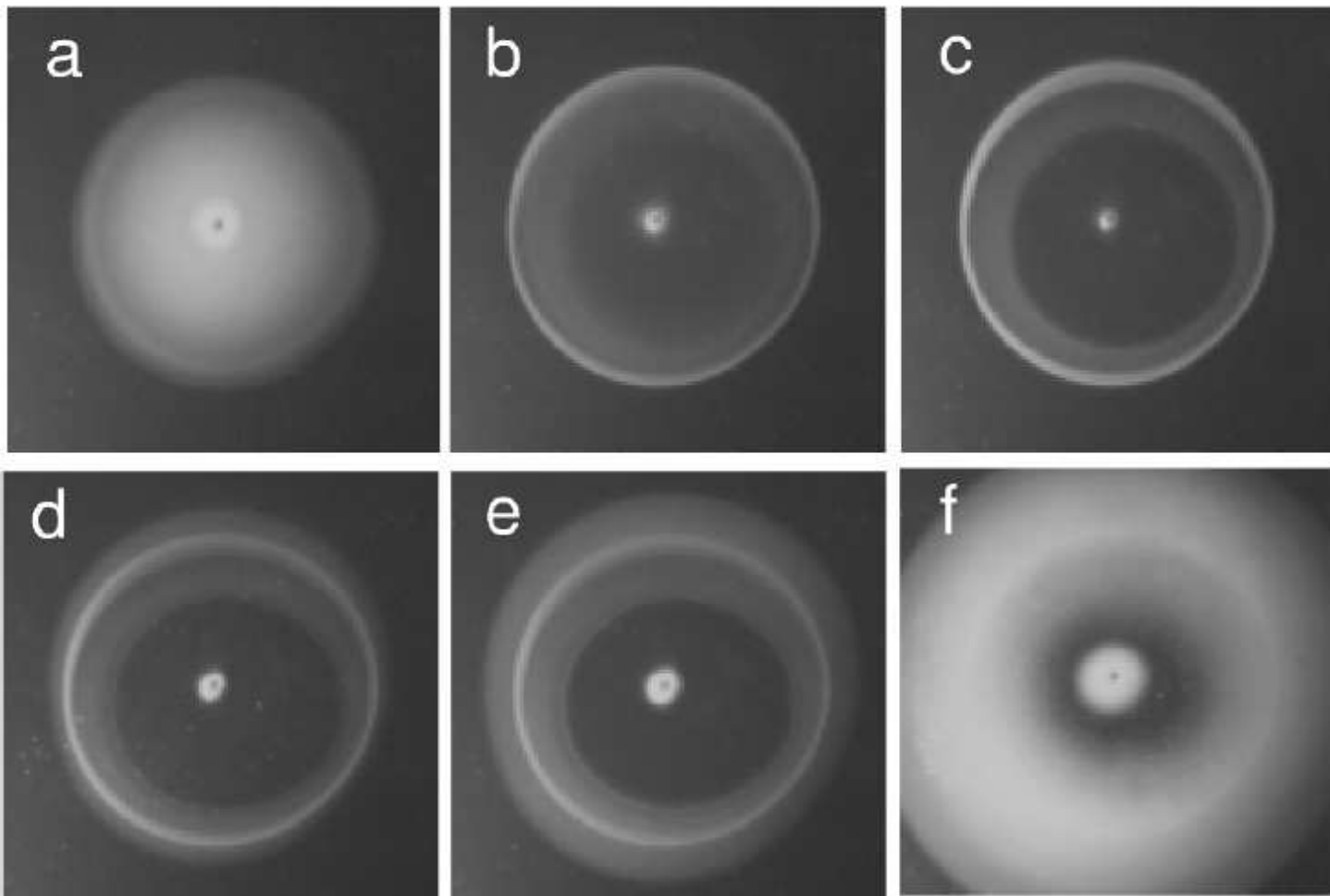
Then K spikes are stable if $K < K_c$. Example: $\alpha = 1, \gamma = 2, \varepsilon = 0.08, D = 1$.



We get $S = 16$, $K_c \approx 10.19$. Starting with random initial conditions, the end state consists of $K = 7.5 < K_c$ hot-spots [counting boundary spots with weight $1/2$ and corner spots with weight $1/4$], in agreement with the theory.

Biological aggregation

- Animals often aggregate in groups
- Biologically, it can provide protection from predators; conserve heat, act without an apparent leader, enable collective behaviour
- Examples include bacteria, ants, fish, birds, bees....









Aggregation model

We consider a simple model of particle interaction,

$$\frac{dx_j}{dt} = \frac{1}{N} \sum_{\substack{k=1, \dots, N \\ k \neq j}} F(|x_j - x_k|) \frac{x_j - x_k}{|x_j - x_k|}, \quad j = 1 \dots N \quad (9)$$

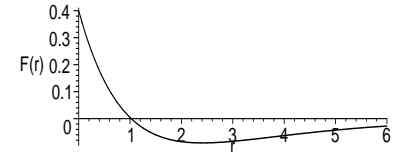
- Models insect aggregation [Edelstein-Keshet et al, 1998] such as locust swarms [Topaz et al, 2008]; robotic motion [Gazi, Passino, 2004].
- Interaction force $F(r)$ is of attractive-repelling type: the insects repel each other if they are too close, but attract each-other at a distance.
- Note that acceleration effects are ignored as a first-order approximation.
- Mathematically $F(r)$ is positive for small r , but negative for large r .
- Alternative formulation: (9) is a gradient flow of the minimization problem

$$\min E(x_1, \dots, x_N) \quad \text{where} \quad E = \sum \sum P(|x_i - x_j|) \quad \text{with} \quad F(r) = -P'(r).$$

Confining vs. spreading

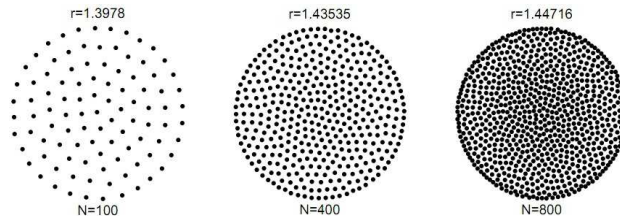
- Consider a **Morse interaction force**:

$$F(r) = \exp(-r) - G \exp(-r/L); \quad G < 1, L > 1$$



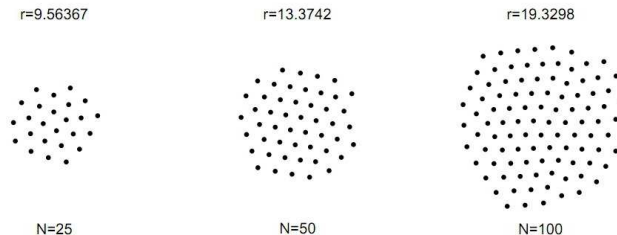
- If $GL^3 > 1$, the morse potential is **confining** (or catastrophic): doubling N doubles the density but cloud volume is unchanged:

$$G = 0.5, \quad L = 2$$



- If $GL^3 < 1$, the system is **non-confining** (or h-stable): doubling N doubles the cloud volume but density is unchanged:

$$G = 0.5, \quad L = 1.2$$



Continuum limit

- For confining potentials, we can take the continuum limit as the number of particles $N \rightarrow \infty$.

- We define the **density** ρ as

$$\int_D \rho(x) dx \approx \frac{\text{\#particles inside domain } D}{N}$$

- The flow is then characterized by density ρ and velocity field v :

$$\rho_t + \nabla \cdot (\rho v) = 0; \quad v(x) = \int_{\mathbb{R}^n} F(|x - y|) \frac{x - y}{|x - y|} \rho(y) dy. \quad (10)$$

- Variational formulation: Let

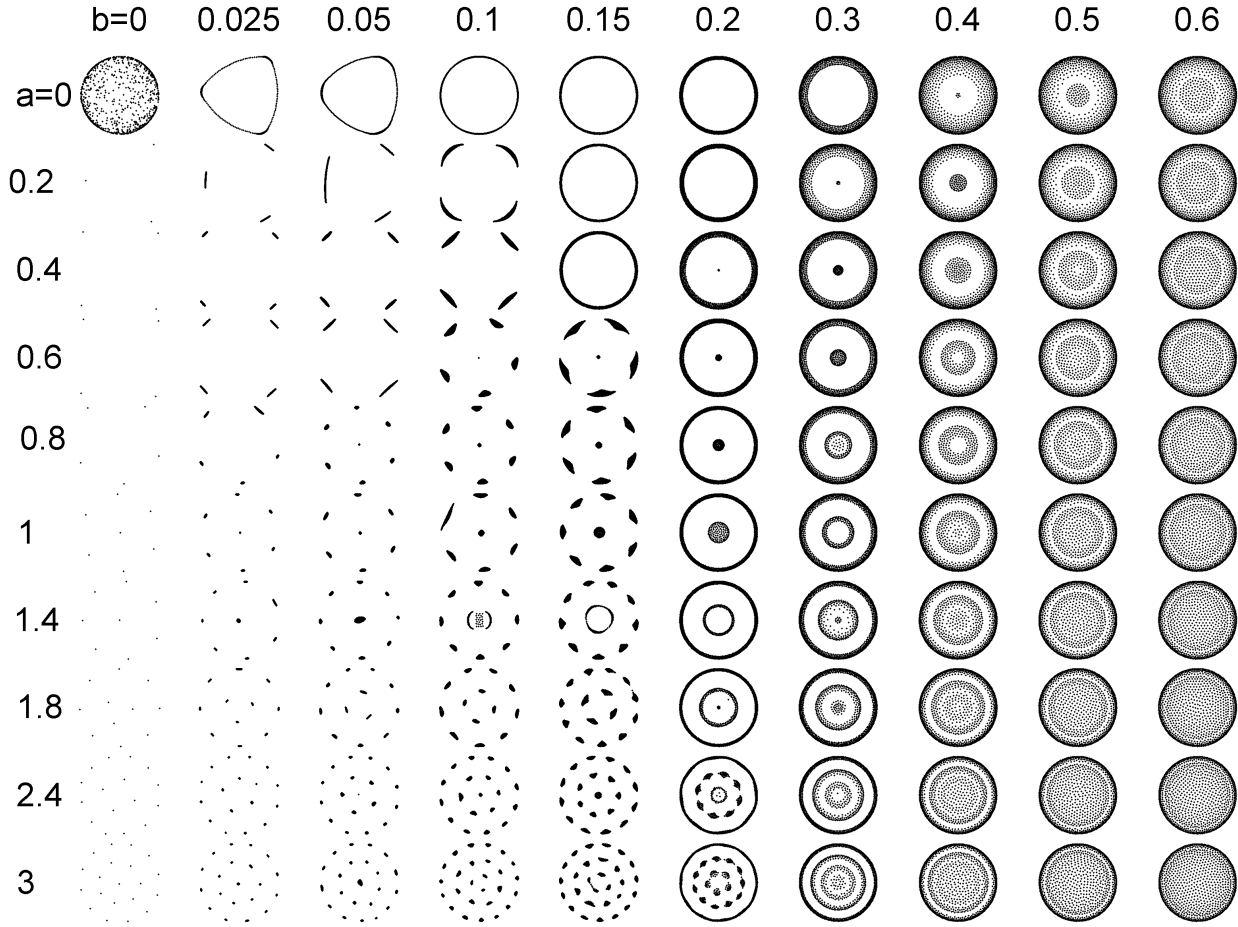
$$E[\rho] := \int_{\mathbb{R}^n} \int_{\mathbb{R}^n} \rho(x) \rho(y) P(|x - y|) dx dy; \quad P'(r) = -F(r) \quad (11)$$

Then (10) is the gradient flow of E ; minima of E are stable equilibria of (10).

- Questions

1. Describe the equilibrium cloud shape in the limit $t \rightarrow \infty$
2. What about dynamics?

Linear force: $F(r) = \min(ar + b, 1 - r)$



Ring-type steady states

- Seek steady state of the form $x_j = r (\cos (2\pi j/N), \sin (2\pi j/N))$, $j = 1 \dots N$.
- In the limit $N \rightarrow \infty$ **the radius of the ring must be the root of**

$$I(r) := \int_0^{\pi/2} F(2r \sin \theta) \sin \theta d\theta = 0. \quad (12)$$

- For Morse force $F(r) = \exp(-r) - G \exp(-r/L)$, such root exists whenever $GL^2 > 1$ [coincides with 1D catastrophic regime]
- For general repulsive-attractive force $F(r)$, a ring steady state exists if $F(r) \leq C < 0$ for all large r .
- Even if the ring steady-state exists, the time-dependent problem can be ill-posed!

Local stability of a ring

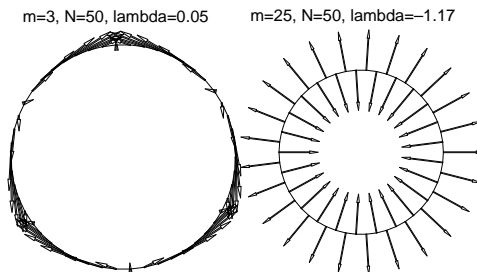
- Linearize: $x_k = r_0 \exp(2\pi i k/N) (1 + \exp(t\lambda)\phi_k)$ where $\phi_k \ll 1$.
- Ring is stable if $\text{Re}(\lambda) \leq 0$ for all pair (λ, ϕ) . There are three zero eigenvalues corresponding to rotation and translation invariance; all other eigenvalues come in pairs due to rotational invariance.
- [K-Hui-Uminsky-Bertozzi] λ is the eigenvalue of

$$M(m) := \begin{bmatrix} I_1(m) & I_2(m) \\ I_2(m) & I_1(-m) \end{bmatrix}; \quad m = 2, 3, \dots \quad (13)$$

$$I_1(m) = \frac{2}{\pi} \int_0^{\pi/2} \left[\frac{F(2r \sin \theta)}{2r \sin \theta} + F'(2r \sin \theta) \right] \sin^2((m+1)\theta) d\theta; \quad (14a)$$

$$I_2(m) = \frac{2}{\pi} \int_0^{\pi/2} \left[\frac{F(2r \sin \theta)}{2r \sin \theta} - F'(2r \sin \theta) \right] [\sin^2(m\theta) - \sin^2(\theta)] d\theta. \quad (14b)$$

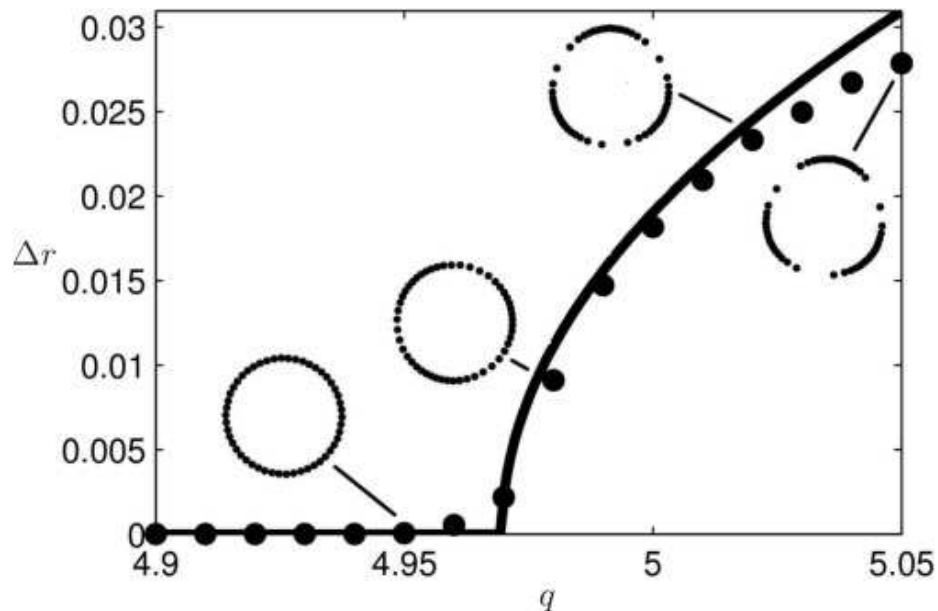
- Eigenfunction is a pure fourier mode when projected to the curvilinear coordinates of the circle.



Triangular shapes: weakly nonlinear analysis

- Near the instability threshold, higher-order analysis shows a **supercritical pitchfork bifurcation**, whereby a ring solution bifurcates into an m -symmetry breaking solution
- This shows existence of nonlocal solutions.
- Example: $F(r) = r^{1.5} - r^q$; bifurcation $m = 3$ occurs at $q = q_c \approx 4.9696$; nonlinear analysis predicts

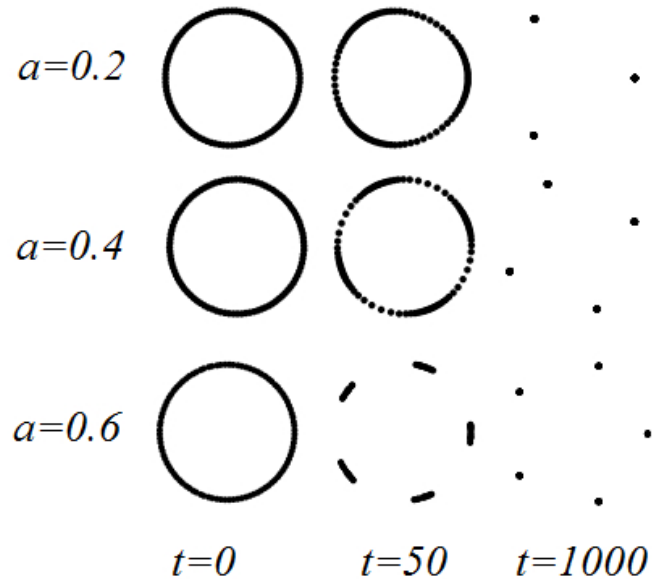
$$\max_i |x_i| - \min_i |x_i| = \sqrt{\max(0, \tau(q - q_c))}; \quad \tau \approx 0.109.$$



Point-concentration (hole) solutions

$$F(r) = \min(ar, r - r^2)$$

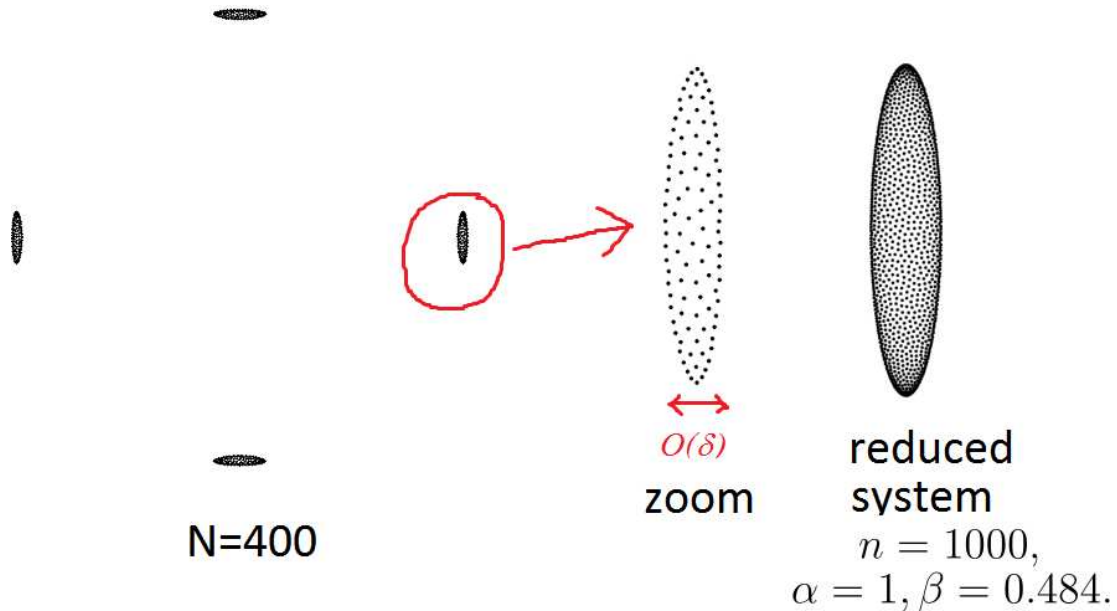
Solutions consist of K “clusters”, where each cluster has N/K points inside. The number K depends on a :



Spots: “degenerate” holes

$$F(r) = \min(ar + \delta, 1 - r); \quad \delta \ll 1$$

- Points degenerate into spots of size $O(\delta)$. eg. $a = 0.3, \delta = 0.05$:



- Inside each of the cluster, the **reduced** problem is:

$$\phi'_l = \sum_{j \neq l}^n \frac{\phi_l - \phi_j}{|\phi_l - \phi_j|} - n \begin{bmatrix} \alpha & 0 \\ 0 & \beta \end{bmatrix} \phi_l$$

- α, β depend only on $F(r)$ not on N .

Annulus: continuum limit $N \gg N_c$:

- $F(r) = r - r^2 + \delta$, $0 < \delta \ll 1$
- **Main result:** In the limit $\delta \rightarrow 0$, the annulus inner and outer radii R_1, R_2 are given by

$$R \sim \frac{3\pi}{16} + \frac{2}{\pi}\delta; \quad R_1 \sim R - \beta, \quad R_2 \sim R + \beta$$

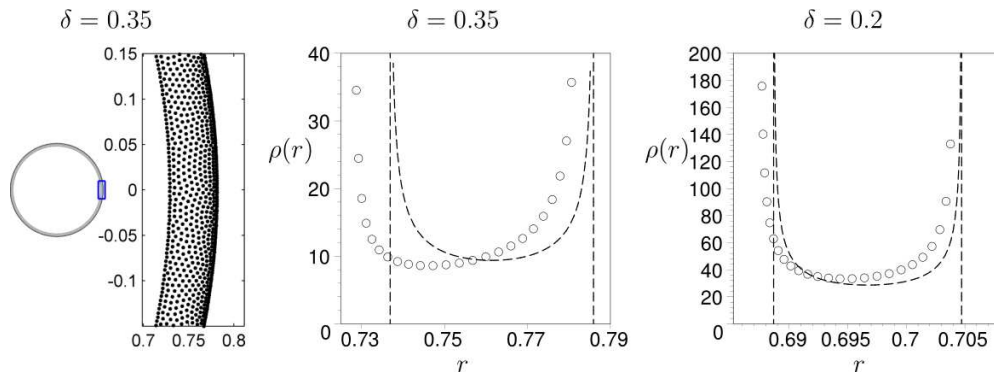
where

$$\beta \sim 3\pi e^{-5} \exp\left(-\frac{3\pi^2}{64} \frac{1}{\delta}\right) \ll \delta \ll 1.$$

The radial density profile inside the annulus is

$$\rho(x) \sim \begin{cases} \frac{c}{\sqrt{\beta^2 - (R - |x|)^2}}, & |R - x| < \beta \ll 1 \\ 0, & \text{otherwise} \end{cases}$$

- Annulus is **exponentially thin in** δ ... note the 1/sqrt singularity near the edges!



Key steps for computing annulus profile

- For radially symmetric density, the velocity field reduces to a 1D problem:

$$v(r) = \int_0^\infty K(s, r) \rho(s) s ds$$

where

$$K(s, r) := \int_0^{2\pi} (r - s \cos \theta) f\left(\sqrt{r^2 + s^2 - 2rs \cos \theta}\right) d\theta; \quad f(r) = 1 - r + \frac{\delta}{r}$$

- Assume thin annulus; expand all integrals. **It boils down to** integral equation (Carleman's equation)

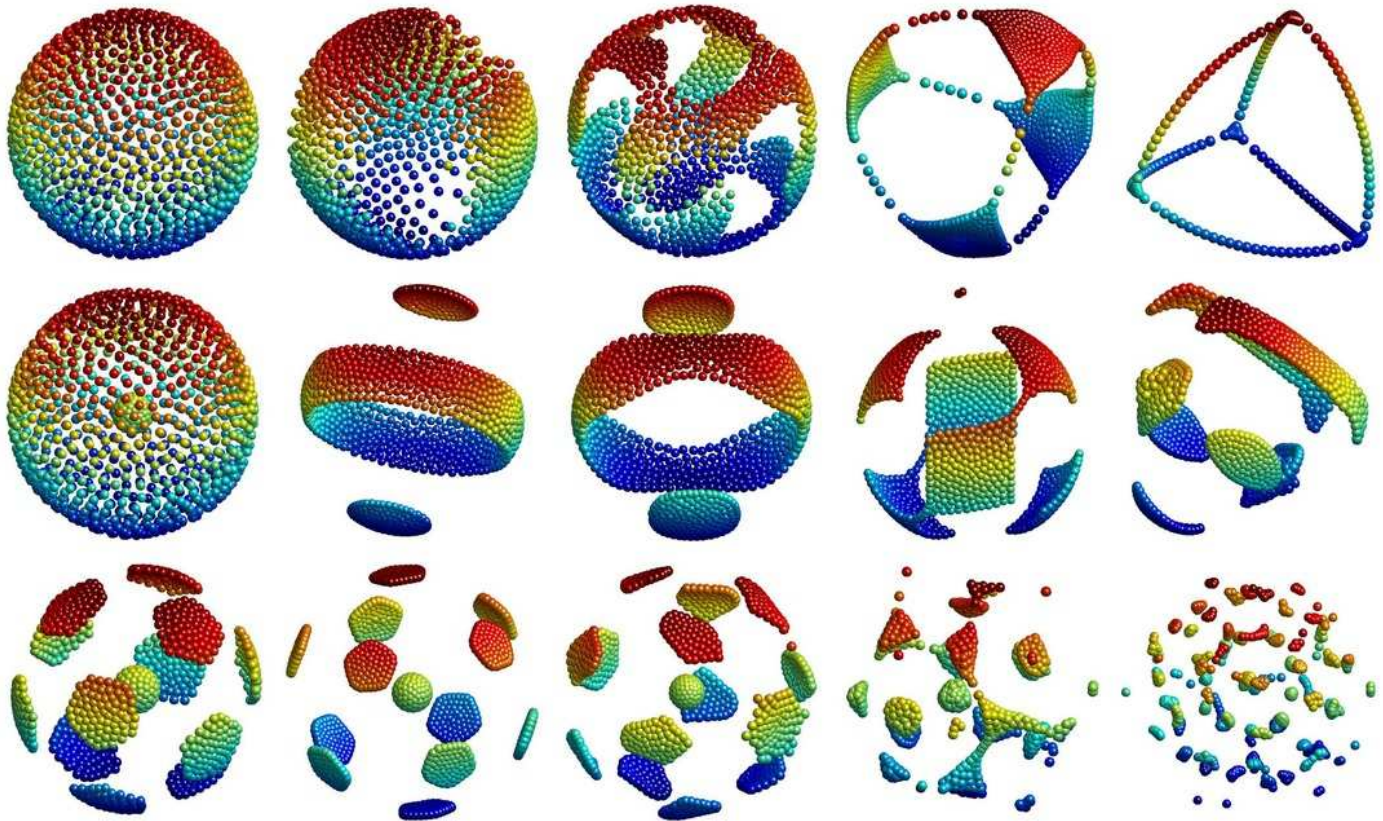
$$\int_{-\beta}^{\beta} \ln |\eta - \xi| \varrho(\eta) d\eta = 1 \quad \text{for all } \xi \in (\alpha, \beta)$$

- **Explicit solution** is a special case of Formula 3.4.2 from “Handbook of integral equations” A.Polyanin and A.Manzhirov:

$$\varrho(\xi) = \frac{C}{\sqrt{\beta^2 - \xi^2}}$$

3D sphere instabilities

- Radius satisfies: $\int_0^\pi F(2r_0 \sin \theta) \sin \theta \sin 2\theta = 0$
- [Von Brecht, Uminsky, K, Bertozzi] Instability is fully characterized using spherical harmonics and hypergeometric functions



Stability of a spherical shell

Define

$$g(s) := \frac{F(\sqrt{2s})}{\sqrt{2s}};$$

The spherical shell has a radius given implicitly by

$$0 = \int_{-1}^1 g(R^2(1-s))(1-s)ds.$$

Its stability is given by a sequence of 2x2 eigenvalue problems

$$\lambda \begin{pmatrix} c_1 \\ c_2 \end{pmatrix} = \begin{pmatrix} \alpha + \lambda_l(g_1) & l(l+1)\lambda_l(g_2) \\ \lambda_l(g_2) & \frac{l(l+1)}{R^2}\lambda_l(g_3) \end{pmatrix} \begin{pmatrix} c_1 \\ c_2 \end{pmatrix}, \quad l = 2, 3, 4, \dots$$

where

$$\lambda_l(f) := 2\pi \int_{-1}^1 f(s)P_l(s) ds;$$

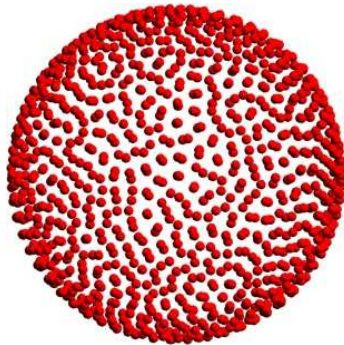
with $P_l(s)$ the Legendre polynomial and

$$\begin{aligned} \alpha &:= 8\pi g(2R^2) + \lambda_0(g(R^2(1-s^2))) \\ g_1(s) &:= R^2 g'(R^2(1-s))(1-s)^2 - g(R^2(1-s))s \\ g_2(s) &:= g(R^2(1-s))(1-s); & g_3(s) &:= \int_0^{R^2(1-s)} g(z)dz. \end{aligned}$$

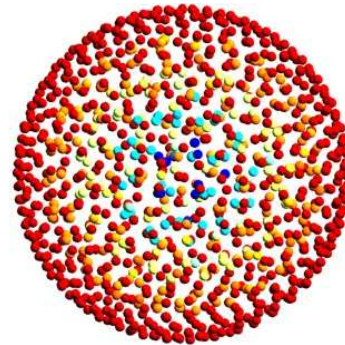
Generalized Lennard-Jones interaction

$$g(s) = s^{-p} - s^{-q}; \quad 0 < p, q < 1; \quad p > q$$

- **MAIN RESULT:** Well posed if $q < \frac{2p-1}{2p-2}$; ill-posed if $q > \frac{2p-1}{2p-2}$.



(a)



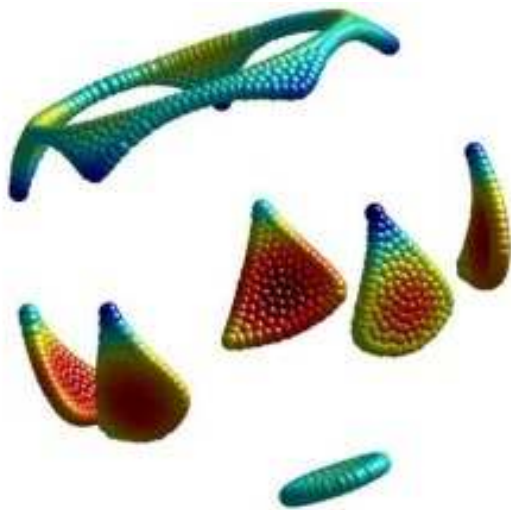
(b)

Example: steady state with $N = 1000$ particles. (a) $(p, q) = (1/3, 1/6)$. Particles concentrate uniformly on a surface of the sphere, with no particles in the interior. (b) $(p, q) = (1/2, 1/4)$. Particles fill the interior of a ball. The particles are color-coded according to their distance from the center of mass.

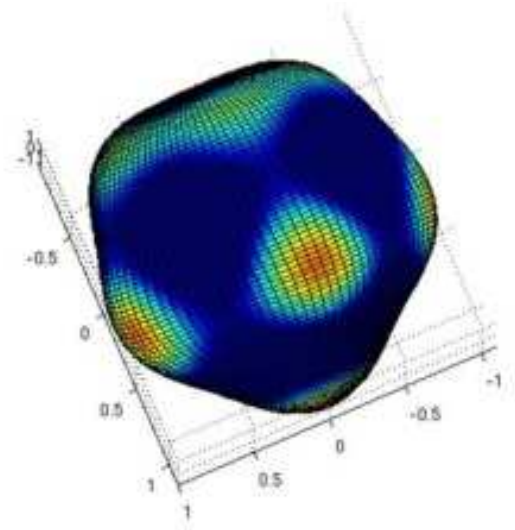
Custom-designed kernels

- In 3D, we can design force $F(r)$ which is stable for all modes except specified mode.
- EXAMPLE: Suppose we want only mode $m = 5$ to be unstable. Using our algorithm, we get

$$F(r) = \left\{ 3 \left(1 - \frac{r^2}{2} \right)^2 + 4 \left(1 - \frac{r^2}{2} \right)^3 - \left(1 - \frac{r^2}{2} \right)^4 \right\} r + \varepsilon; \quad \varepsilon = 0.1.$$



Particle simulation



Linearized solution

Part II: Constant-density swarms

- Biological swarms have sharp boundaries, relatively **constant internal population**.
- Question: *What interaction force leads to such swarms?*
- More generally, can we deduce an interaction force from the swarm density?



Bounded states of constant density

Claim. Suppose that

$$F(r) = \frac{1}{r^{n-1}} - r, \quad \text{where } n \equiv \text{dimension}$$

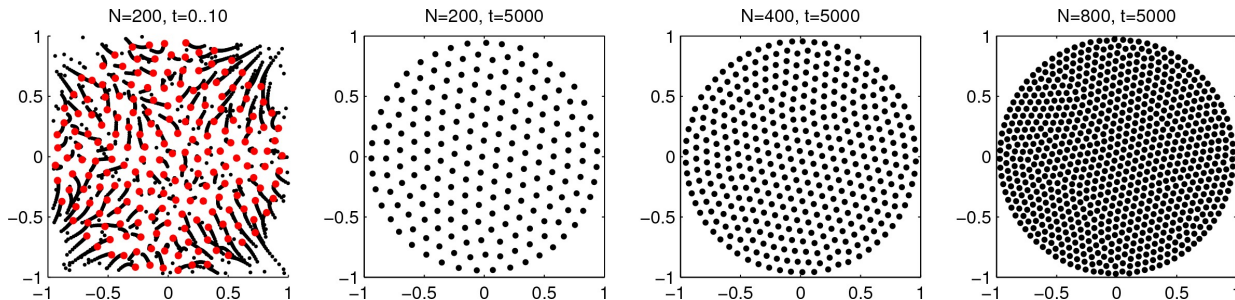
Then the aggregation model

$$\rho_t + \nabla \cdot (\rho v) = 0; \quad v(x) = \int_{\mathbb{R}^n} F(|x - y|) \frac{x - y}{|x - y|} \rho(y) dy.$$

admits a steady state of the form

$$\rho(x) = \begin{cases} 1, & |x| < R \\ 0, & |x| > R \end{cases}; \quad v(x) = \begin{cases} 0, & |x| < 1 \\ -ax, & |x| > 1 \end{cases}.$$

where $R = 1$ for $n = 1, 2$ and $a = 2$ in one dimension and $a = 2\pi$ in two dimensions.



Method of characteristics in 1D

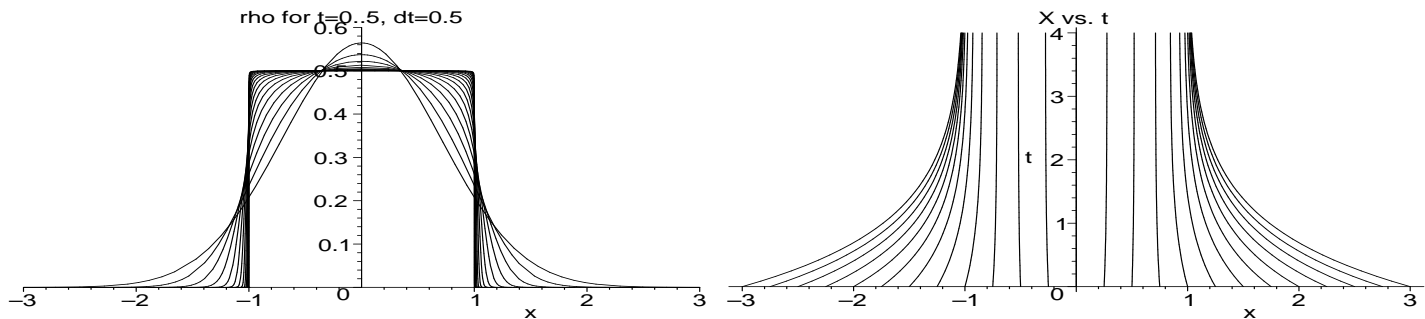
Suppose that $F(r) = 1 - r$. Then

$$X = \frac{2w_0(x_0)}{M} - 1 + e^{-Mt} \left(x_0 + 1 - \frac{2w_0(x_0)}{M} \right)$$

$$w_0(x_0) = \int_{-\infty}^{x_0} \rho_0(z) dz; \quad M = \int_{-\infty}^{\infty} \rho_0(z) dz$$

$$\rho(X, t) = \frac{M}{2 + e^{-tM} (M/\rho_0(x_0) - 2)}$$

Example: $\rho_0(x) = \exp(-x^2) / \sqrt{\pi}$; $M = 1$:



Inverse problem: Custom-designer kernels: 1D

Theorem. In one dimension, consider a radially symmetric density of the form

$$\rho(x) = \begin{cases} b_0 + b_2x^2 + b_4x^4 + \dots + b_{2n}x^{2n}, & |x| < R \\ 0, & |x| \geq R \end{cases} \quad (15)$$

Define the following quantities,

$$m_{2q} := \int_0^R \rho(r)r^{2q}dr. \quad (16)$$

Then $\rho(r)$ is the steady state corresponding to the kernel

$$F(r) = 1 - a_0r - \frac{a_2}{3}r^3 - \frac{a_4}{5}r^5 - \dots - \frac{a_{2n}}{2n+1}r^{2n+1} \quad (17)$$

where the constants a_0, a_2, \dots, a_{2n} , are computed from the constants b_0, b_2, \dots, b_{2n} by solving the following linear problem:

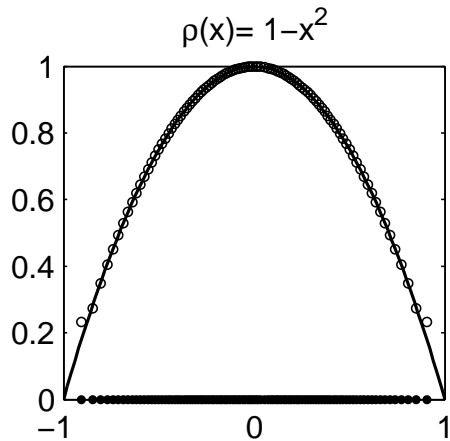
$$b_{2k} = \sum_{j=k}^n a_{2j} \binom{2j}{2k} m_{2(j-k)}, \quad k = 0 \dots n. \quad (18)$$

Example: custom kernels 1D

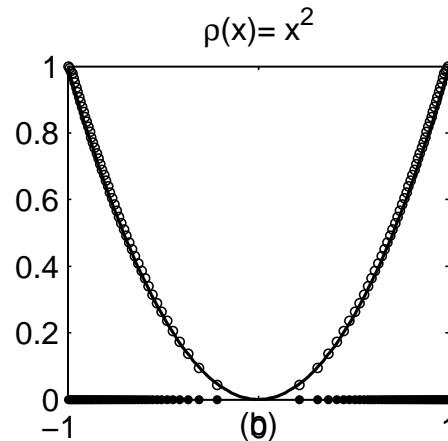
Example 1: $\rho = 1 - x^2$, $R = 1$, then $F(r) = 1 - 9/5r + 1/2r^3$.

Example 2: $\rho = x^2$, $R = 1$, then $F(r) = 1 + 9/5r - r^3$.

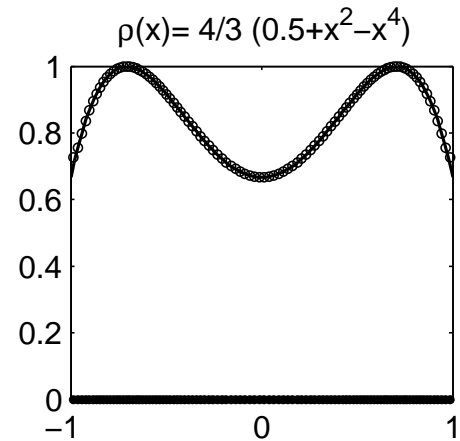
Example 3: $\rho = 1/2 + x^2 - x^4$, $R = 1$; then $F(r) = 1 + \frac{209425}{336091}r - \frac{4150}{2527}r^3 + \frac{6}{19}r^5$.



Ex.1



Ex.2



Ex.3

Inverse problem: Custom-designer kernels: 2D

Theorem. In two dimensions, consider a radially symmetric density $\rho(x) = \rho(|x|)$ of the form

$$\rho(r) = \begin{cases} b_0 + b_2 r^2 + b_4 r^4 + \dots + b_{2n} r^{2n}, & r < R \\ 0, & r \geq R \end{cases} \quad (19)$$

Define the following quantities,

$$m_{2q} := \int_0^R \rho(r) r^{2q} dr. \quad (20)$$

Then $\rho(r)$ is the steady state corresponding to the kernel

$$F(r) = \frac{1}{r} - \frac{a_0}{2} r - \frac{a_2}{4} r^3 - \dots - \frac{a_{2n}}{2n+2} r^{2n+1} \quad (21)$$

where the constants a_0, a_2, \dots, a_{2n} , are computed from the constants b_0, b_2, \dots, b_{2n} by solving the following linear problem:

$$b_{2k} = \sum_{j=k}^n a_{2j} \binom{j}{k}^2 m_{2(j-k)+1}; \quad k = 0 \dots n. \quad (22)$$

This system always has a unique solution for provided that $m_0 \neq 0$.

Numerical simulations, 2D

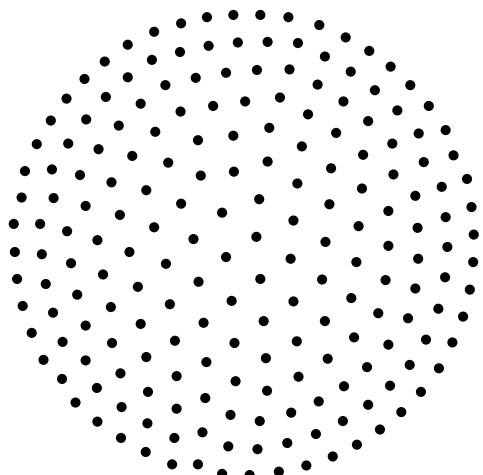
- Solve for x_i using ODE particle model as before [$2N$ variables]
- Use x_i to compute **Voronoi diagram**;
- Estimate $\rho(x_j) = 1/a_j$ where a_j is the area of the voronoi cell around x_j .
- Use **Delanay triangulation** to generate smooth mesh.
- **Example:** Take

$$\rho(r) = \begin{cases} 1 + r^2, & r < 1 \\ 0, & r > 0 \end{cases}$$

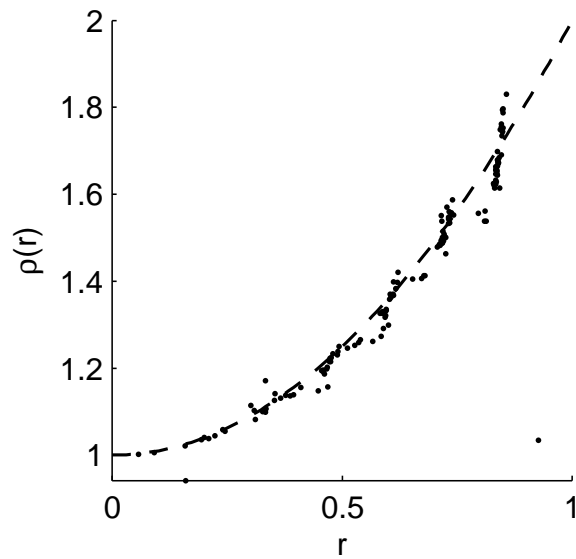
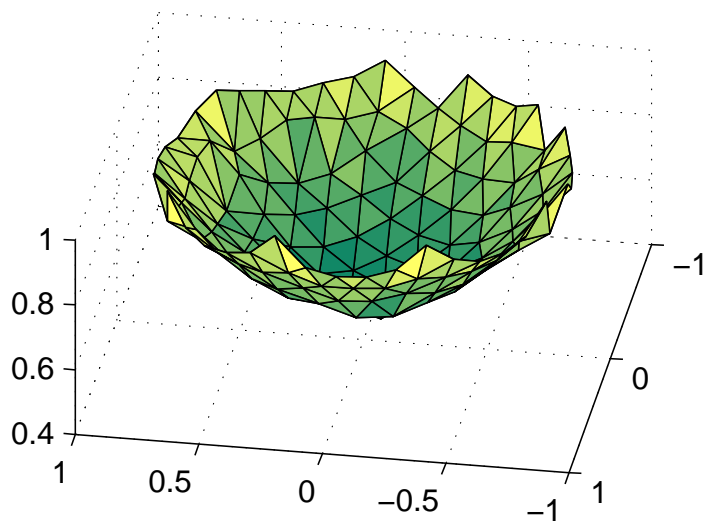
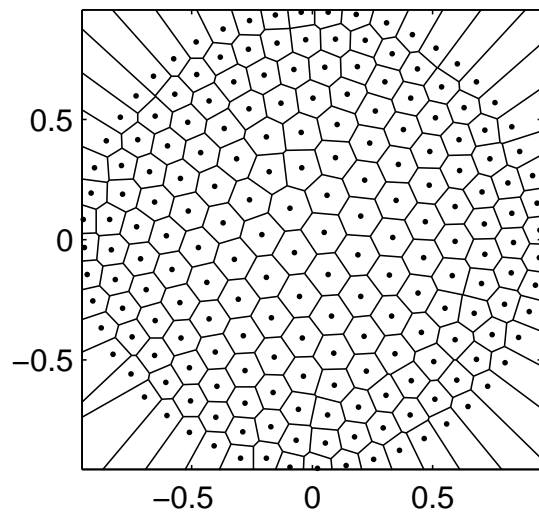
Then by Custom-designed kernel in 2D is:

$$F(r) = \frac{1}{r} - \frac{8}{27}r - \frac{r^3}{3}.$$

Running the particle method yeids...



$R=0.955484$



Conclusions

- Analysis of localized patterns requires many different tools: asymptotic methods, complex variables, dynamical systems, special functions, numerical methods,
- Has many relevant applications in science, but also leads to beautiful mathematics
- Many good problems suitable for students at all levels
- This talk and related papers are downloadable from my website
<http://www.mathstat.dal.ca/~tkolokol/papers>

Thank you!